Composite Structures 340 (2024) 118174

Contents lists available at ScienceDirect

Composite Structures

journal homepage: www.elsevier.com/locate/compstruct

Effects of long-term exposure of NSM CFRP-to-concrete bond to natural and accelerated aging environments

Aloys Dushimimana [a], José Sena-Cruz [a,*], Luís Correia [a], João Miguel Pereira [a], Susana Cabral-Fonseca [b], Ricardo Cruz [a]

[a] University of Minho, ISISE/IB-S, ARISE, Department of Civil Engineering, Guimarães, Portugal
[b] National Laboratory for Civil Engineering, Materials Department, Lisbon, Portugal

ARTICLE INFO

Keywords:
Durability
Natural aging
Accelerated aging
NSM CFRP-to-concrete bond
Epoxy adhesive
Concrete
Carbon fiber

ABSTRACT

Carbon fiber reinforced polymer (CFRP) composites can be used to strengthen existing reinforced concrete (RC) structures. The CFRP laminate can be bonded to RC structure using epoxy adhesive via near-surface mounted (NSM) strengthening technique. However, existing literature generally lacks data about durability of NSM CFRP-to-concrete bond. In this study, strengthened concrete elements were exposed to laboratory-controlled environments (at approximately 20 °C/55 % RH, and water immersion at 20 °C) and natural field environments (to promote natural aging induced mainly by carbonation, high temperatures, freeze–thaw attack, and airborne chlorides) for up to four years. Durability tests were conducted yearly for the bond and its constituent materials. The highest bond strength degradations were nearly 12 % and 9 % for the specimens immersed in water and those exposed to freeze–thaw attack, respectively. Besides, environmental conversion factors of 0.88 and 0.93 were derived from a database of existing accelerated, and natural aging data from the present work, respectively.

1. Introduction

It is undoubtedly realistic to state that concrete has been proven to be a reliable construction material since its invention. Concrete has very good compressive behavior but generally poor tension properties; however, it can usually be reinforced with e.g., steel bars to become reinforced concrete (RC) with improved tensile properties. This constructive solution has been used for several decades and the growing need to extend and/or maintain the service life of these structures has led to significant investments in the strengthening of RC structures. Fiber Reinforced Polymer (FRP) composites can be used to strengthen RC structures. In particular, carbon FRP (CFRP) can be a good option, owing to its advantageous properties including high strength to weight ratio, high durability, high fatigue resistance [1], and high corrosion resistance [2], among others. CFRP composites in the form of laminate strips and sheets have generally been applied for flexural and shear strengthening of existing RC structures, respectively, where a bonding agent, such as epoxy adhesive, is typically used to bond the CFRP to concrete substrate. Near-surface mounted (NSM) is known as one of the existing strengthening techniques [3], and its durability is mainly addressed in the present work. During application of the NSM technique, the CFRP strip is basically inserted into a groove pre-cut on concrete cover [4], and is bonded to concrete with an adhesive. The NSM technique is more recent and has been repeatedly reported to possess more advantages than other techniques, such as, the externally bonded reinforced (EBR) technique [5–8]. Furthermore, NSM can additionally be prestressed, mainly to benefit from the full usage of the CFRP strain, which leads to efficient use of materials, thereby resulting in reduced crack width and increased cracking and yield response [9,10]. However, the durability of the bond in NSM technique, either non-prestressed or prestressed, still lacks literature under both accelerated aging test (AAT) and natural aging test (NAT) protocols. Besides, the durability of the materials constituting the bond in NSM technique (i.e., concrete, epoxy adhesive, and CFRP) has also not been fully investigated yet, considering NAT protocols (e.g., [11,12]), thus there is a need to conduct further related research.

A significant number of studies have been conducted on the AAT of the NSM–to-concrete bond constituent materials. Starting from concrete, carbonation of concrete is an important durability factor. Studies show that high temperatures can make concrete more porous thereby leading to carbonation depth increase, which thereafter can improve concrete properties [13–15], although the carbonation is known to have

* Corresponding author.
E-mail address: jose.sena-cruz@civil.uminho.pt (J. Sena-Cruz).

https://doi.org/10.1016/j.compstruct.2024.118174
Received 9 January 2024; Received in revised form 21 March 2024; Accepted 3 May 2024
Available online 5 May 2024

negative effects on the reinforcing steel bar [16]. In contrast, low temperatures and high relative humidity (RH) [17], as well as continuous cement hydration (leading to micropore closure) [18] can hinder the carbonation depth increase. On the other hand, carbonation depth can be high if concrete is exposed to environments with 50–70 % RH [13] (the optimum increase being at 65 % RH [17]). In a study by [19], both concrete elastic modulus and compressive strength increased after carbonation. Besides, only the compressive strength of concrete increased after exposure to carbonation in [18], and to ultraviolet (UV) radiation at certain humidity and temperature in [20]. Studies have also shown that when concrete is exposed to both carbonation and chlorides, the carbonation can release bound chlorides inward at greater depths [21,22], thereby minimizing the effects of chlorides at the concrete surface and hence protecting the concrete surface region, where FRP is normally bonded during strengthening applications.

In studies addressing the durability of epoxy adhesives, it has been found that the properties of the adhesives reduce significantly after exposure to moisture or in the case of full immersion in water [11,23]. Wet-dry cycles were also found to decrease both the tensile strength and elastic modulus of the adhesive [24]. However, exposure to high temperatures improved the adhesive properties through post-curing phenomenon [25], while temperatures close to the glass transition temperature resulted in softening of the polymeric matrix [11]. Besides, high carbonation can accelerate the curing of the epoxy resin [26]. However, exposure of the adhesive to chlorides has no harmful effect on the adhesive properties [27].

Regarding the durability of CFRP composites, studies show that CFRP is generally not affected by degradation agents such as chloride exposure [11], and thermal cycles (TC) in air [28]. However, freeze–thaw (FT) cycles may reduce both tensile strength and elongation of CFRP [29], UV radiation can affect a few microns from the CFRP surface [30], and some polymeric matrix microcracks may form due to different thermal expansion coefficients between the fiber and matrix after exposure to TC.

It is worth noting that existing literature on the durability of the bond constituent materials has generally been conducted using AAT protocols and basically addresses the effect of a single degradation agent; however, in outdoor environment the materials are exposed to more than one degradation agent simultaneously. Hence there is a need to conduct studies that address the combined or synergic effect of different agents to be able to mimic what normally occurs in outdoor environments.

Regarding the NSM CFRP-to-concrete bond, there are some studies [7,31–33] that address the durability of the bond under AAT conditioning. In [31], 90 wet-dry cycles lasting for 2160 h were applied on strengthened concrete elements with 60 mm and 90 mm bond lengths, 1.4 mm CFRP laminate thickness,15 mm and 25 mm groove depths, and 4 mm and 8 mm groove widths. The bond strength generally decreased after exposure, except for specimens with 25 mm groove depth and 4 mm groove width. In [33], conditioning specimens to 300 freeze–thaw cycles or immersion in salt water at 20 °C decreased the bond strength for concrete elements strengthened with a 1.3 mm CFRP laminate thickness. In [7], immersion in tap water at 22 °C (or tap water with 3.5 NaCl) for 5760 h and 11,520 h increased the bond strength of concrete elements strengthened with 1.4 mm CFRP laminate thickness. Furthermore, applying 240 or 480 wet-dry cycles on the specimens in tap water (or in tap water with 3.5 NaCl) also increased the bond strength. Besides, conditioning the specimens with temperature cycles between −15 °C and + 60 °C increased the bond strength; however, temperature cycles between + 20 °C and + 80 °C did not affect the bond strength. Finally, conditioning the specimens to 120 freeze–thaw cycles between −18 °C to + 20 °C for 5760 h also did not affect the bond strength, but doubling the number of freeze–thaw cycles between −18 °C to + 20 °C for 4320 h led to a slight decrease in the bond strength. On the other hand, a few studies, e.g., [8,34,35] addressed the durability of NSM with NAT protocols. In these NAT-based studies, it was generally found that the NSM CFRP-to-concrete bond is significantly affected by moisture and freeze–thaw attack.

Based on the above mentioned literature on both the NSM CFRP-to-concrete bond and the material constituting the bond, it can be noted that there is a knowledge gap in several aspects, namely: (i) existing durability data are largely based on the AAT protocols with very little knowledge on the behavior of the bond and materials under real outdoor environments; (ii) existing data, apart from being heavily dependent on the AAT protocols, are still insufficient to lead to appropriate predictions of environmental conversion factors (ECF); and, (iii) currently some standards [36,37] recommend ECFs to account for degradation of epoxy/carbon systems due to some generic exposures; however, these ECFs are neither derived from sufficient data, nor from data including both AAT and NAT protocols. Furthermore, there is no information about the factors for specific types of exposures, which is generally the real situation for most of the RC strengthened structures.

Regarding the above aspects, the present work intends to contribute to increasing the number of existing data related to the durability of NSM CFRP-to-concrete bond and attempt to address the above-mentioned aspects. This is achieved by firstly presenting durability data from AAT (laboratory-controlled environments: specimens conditioned at 20 °C/55 %RH or immersed in water at 20 °C) and NAT (outdoor environments: specimens kept in outdoor regions with characteristics mainly promoting carbonation, elevated temperatures, freeze–thaw attacks, and airborne chlorides) protocols. Secondly, the ECF from a database of existing AAT data and the ECF from NAT data in the present work, are derived and compared.

2. Experimental program

This section first describes the properties of the materials composing the NSM CFRP-to-concrete bond followed by detailing the environments studied, and, finally, the testing methods used.

2.1. Constituent materials

Three different materials involved in the bond of NSM CFRP-to-concrete system are analyzed: the concrete, the epoxy adhesive and the CFRP laminate. Details of each are given below.

Concrete: The concrete used in the preparation of all specimens was in accordance with the recommendations as per [38]. All concrete properties were as shown in Table 1. Concrete cylinders (Fig. 1a) were produced and used to investigate the variation of concrete elastic modulus (E_c) and compressive strength (f_{cc}). Concrete prisms (Fig. 1b) were used to assess the variation of concrete pull-off strength (f_{ct}) and the concrete carbonation depth (C_d).

Epoxy adhesive: A two-component commercial cold-curing epoxy resin-based adhesive with properties as shown in Table 1 was used to cast the dog-bone shaped specimens (Fig. 1c) and to investigate the variation of the adhesive elastic modulus (E_a) and tensile strength (f_a). This adhesive was then used as a bonding agent in NSM CFRP-to-concrete bond specimens. The adhesive is a solvent-free, thixotropic, in grey color, developed for bonding carbon fiber laminates to concrete substrates. The properties of this adhesive according to the supplier [39] are shown in Table 1.

CFRP laminate: The CFRP laminate (Fig. 1d) produced by S&P [40] was used to strengthen the concrete elements and its properties are as shown in Table 1. This CFRP laminate has a rectangular cross-section of 10 mm × 1.4 mm (width × thickness). Besides, the variations of both its elastic modulus (E_f) and tensile strength (f_f) were also investigated using CFRP strips.

NSM CFRP-to-concrete bond: The properties of the specimens used to characterize the bond between the CFRP laminate and concrete are also shown in Table 1.

Table 1
Properties of the NSM CFRP-to-concrete bond specimens and its constituent materials.

Concrete		**Epoxy adhesive**	
Concrete class	C30/37 (cylinder/ cube in [MPa])	Type of adhesive	Cold-curing S&P Resin 220
Max aggregate size [mm]	12.5	Density, at 23 °C [g/ cm^3]	1.7–1.8
Cement type	CEM II/A–L 42.5R	Flexural elastic modulus [GPa]	> 7.1
Slump [mm]	160–210 (slump class S4)	Tensile strength [MPa]	19.9 (after 7d curing at 20 °C)
Water-to-cement ratio	0.4	Glass transition temperature [T_g] in °C	46.2 (after 7d curing at 23 °C)
Exposure class	XC4(P)	Compressive strength [MPa]	> 70
E_c [GPa]	29.1 (at 28 days)	Shear strength [MPa]	> 26
f_{cc} [MPa]	41.5 (at 28 days)	*BS* by pull-off, on concrete [MPa]	3 (after 3d curing at 20 °C)
CFRP laminate		**CFRP-to-concrete bond**	
Type and trademark	S&P clever (CFK 150/2000)	CFRP cross-section [mm^2]	10 × 1.4
Prefabricated by	Pultrusion	Concrete cube dimensions [mm^2]	200 × 200
Fiber orientation	Unidirectional	Bond length [mm]	60
Fiber content [%]	68	Groove depth [mm]	15
Fiber matrix	Vinyl ester resin (with $T_g \approx 85^{\circ}$ C)	Groove width [mm]	5
External surface	Black, smooth	Epoxy adhesive thickness [mm]	5 / 3.6 at the CFRP level
Elastic modulus [GPa]	> 170	Epoxy adhesive depth [mm]	15
Tensile strength [MPa]	> 2000	Type of test	Single-lap shear test

Notes: f_{cc}: average compressive strength; E_c: average elastic modulus; *BS*: bond strength; T_g: glass transition temperature; 3d: three days; 7d: seven days.

2.2. Environmental exposure conditions

Six different environmental exposure conditions (E1-E6) were used to study the degradation of both the NSM CFRP-to-concrete bond and its constituent materials. Different characterization tests were performed on the specimens before exposure (referred to as T0) and on the specimens collected from the different environments after one year (T1), two years (T2), three years (T3) and four years (T4) of exposure. Description of the exposure conditions in each environment is provided as follows.

2.2.1. Laboratory-controlled environments

Two laboratory-controlled environments were considered. In the first environment, denoted as E1, the specimens were kept in an in-house walk-in climatic chamber with a targeted temperature and relative humidity of 20 °C and 55 % RH, respectively. The second environment, denoted as E2, consisted of specimens fully and continuously immersed in water at 20 °C (see Fig. 2a and Fig. 2b). The specimens in E2 were tested under wet state. More details about these two environments can be found in [8,11].

2.2.2. Natural outdoor environments

Four different outdoor environments were selected in different regions of Portugal with different meteorological conditions. These environments were selected with the aim of promoting the degradation of the NSM CFRP-to-concrete bond and its constituent materials. The first outdoor environment, denoted as E3, was chosen to mainly promote concrete carbonation, by exposing the specimens to air pollution (all along the year) from highway with heavy traffic and the international airport of Lisbon. The second environment (E4) was chosen to mainly promote the freeze–thaw attacks, and therefore, the specimens were placed on the highest mountain of Portugal (at the altitude of 1600 m) with some seasonal snowfall. The third environment (E5) was chosen to mainly promote the degradation due to high temperatures, so the specimens were placed in a region with yearly elevated temperatures (Fig. 2c and Fig. 2d). The fourth environment (E6) was selected just close to the Atlantic Ocean to promote airborne chloride attack, and the effects of high seasonal humidity.

Although these outdoor environments were chosen to primarily promote the mentioned degradation agents, the specimens kept outdoors are likely to be affected by more than one degradation agent. For example, in E3, in addition to carbonation, high temperatures can also play an important role as the region generally experiences hot weather throughout the year. Typical variations in temperature and relative humidity in the laboratory and outdoor environments are shown in Fig. 3. Particularly, in E1, the relative humidity varies in the range of 45–77 % RH, which promotes concrete carbonation [13,17]. The RH variations are mainly due to inevitable opening/closing of the door of the climatic chamber for maintenance and data collection and fall within the moderate humidity range (exposure class XC3), according to

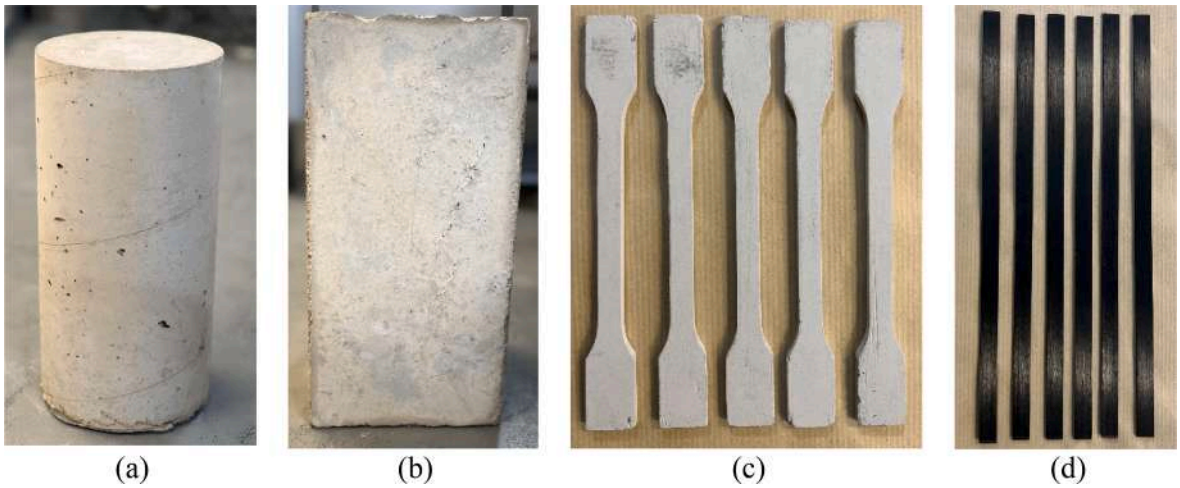

Fig. 1. NSM CFRP-to-concrete bond constituent materials: (a) concrete cylinder, (b) concrete prism, (c) epoxy adhesive dog bone shaped specimens and (d) CFRP laminate strips.

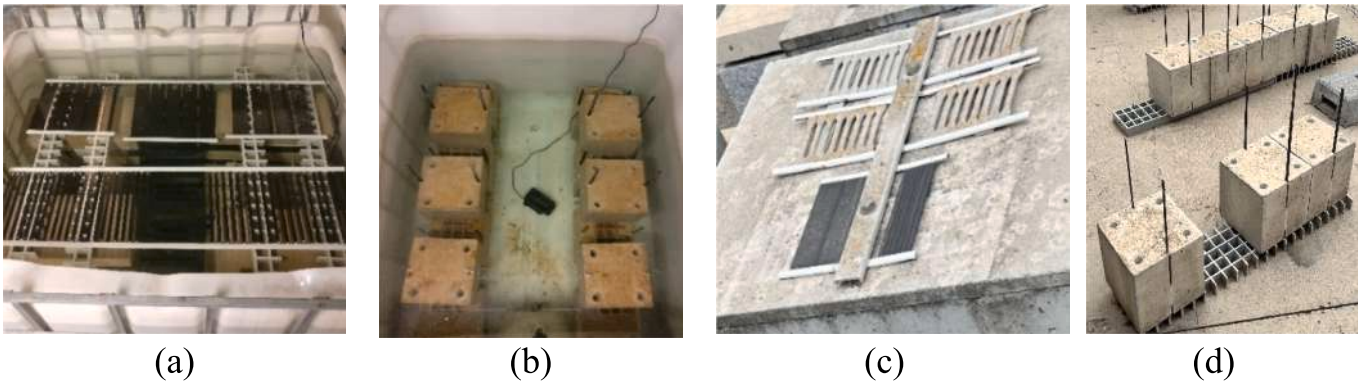

Fig. 2. Typical examples of studied environments: (a) exposure of the constituent materials specimens to water immersion (concrete, epoxy adhesive and CFRP laminate); (b) exposure of the specimens of NSM CFRP-to-concrete bond to water immersion (E2); exposure of (c) constituent materials and (d) NSM CFRP-to-concrete bond specimens to natural outdoor environments (E5).

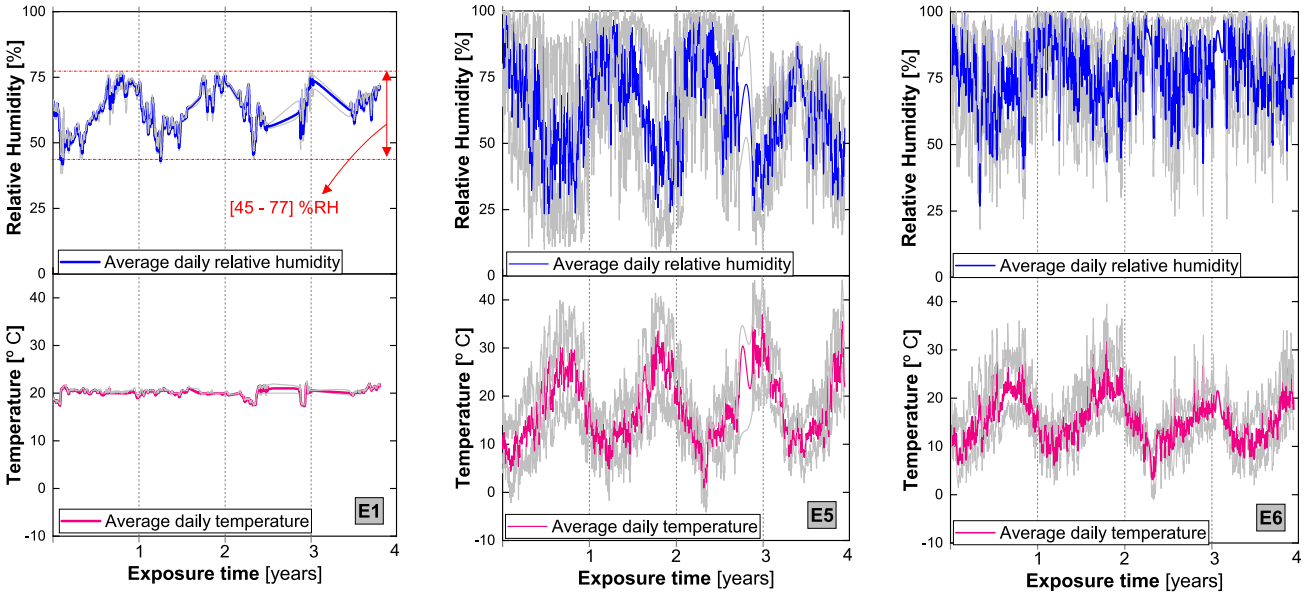

Fig. 3. Typical meteorological records from laboratory (E1) and outdoor (E5, E6) environments.

the Eurocode 1992–1-1:2004 (E) [41]. These actions may have promoted the flow of CO_2 from the laboratory environment into the climate chamber. Furthermore, a significant difference in terms of temperature and relative humidity can also be observed in outdoor environments (E4 and E5). More details can be found in [42], where a general view is that E4 and E6 tend to experience low temperatures and high relative humidity; while E3 and E5 experience high temperatures and low relative humidity. The variation of annual temperatures and relative humidity is tabulated in Table 2, where it can be noted that the maximum temperatures from E3 and E5 were the highest, as expected due to their high daily temperatures as compared to other environments.

2.3. Characterization test methods

This section provides information about the tests adopted for the characterization of both the NSM CFRP-to-concrete bond and its constituent materials. In all the cases, specimens were tested before ageing (T0) and after being exposed to the environments during one (T1), two (T2), three (T3) and fours (T4) years. In the case of environment E2, all the specimens were tested in wet state.

2.3.1. Concrete

A universal testing machine (UTM) with a maximum load capacity of 2000 kN was used to perform compression tests for the concrete elastic modulus (E_c) and compressive strength (f_{cc}). Under non-destructive test (Fig. 4a), three LVDTs spaced at 120° were used to measure the data required to estimate the E_c according to EN 12390–13:2013 [43]. Furthermore, a destructive test (Fig. 4b) was performed on the same specimen to determine the f_{cc} according to NP EN 12390–3:2011 [44]. A total of 75 specimens were tested to determine both the E_c and the f_{cc}. Additionally, the pull-off test was performed using the DYNA Z5 testing machine according to EN 1542:1999 [45]. After allowing the epoxy adhesive to cure for 7 days at room temperature, metal dollies bonded to the concrete cores (using the epoxy adhesive) were manually loaded (Fig. 4c) to pull-off the formed cylinder, until the cylinder' split occurred (Fig. 4d). A total of 100 specimens were tested (series of 4 tests). Further details of this type of test can be found in [8].

In addition to these tests, the carbonation ingress of concrete was also evaluated by spraying phenolphthalein indicator on the cylindrical cores drilled from concrete prisms (series of 4 specimens). After spraying, the clear areas of the specimens indicated the concrete carbonated areas, while the purple-red areas indicated the concrete non-carbonated areas. These tests were performed according to [8], to measure the

Table 2
Variation of annual temperatures and relative humidity in the studied environments.

Variable / Environment		E1	E2	E3	E4	E5	E6
Temp [°C]	Max	20.2 (22.5)	20.2 (20.3)	23.1 (46.2)	17.8 (32.4)	24.0 (44.6)	21.6 (36.0)
Year 1 (T1)	Min	19.8 (13.5)	20.1 (19.0)	13.4 (3.3)	11.1 (−4.7)	11.1 (−1.9)	11.8 (1.5)
	Avg	19.9	20.0	17.4	14.3	17.4	16.15
RH [%]	Max	62.8	100.0	87.9	83.3	84.9	88.7
Year 1 (T1)		(79.5)		(100.0)	(100.0)	(100.0)	(100.0)
	Min	57.8 (31.0)	100.0	48.8 (11.0)	50.9 (4.0)	40.3 (9.0)	59.8 (18.0)
	Avg	60.0	100.0	70.7	67.2	63.5	76.1
Temp [°C]	Max	20.4 (22.0)	20.2 (20.4)	22.7 (39.7)	14.0 (29.6)	23.6 (39.9)	22.5 (39.5)
Year 2 (T2)	Min	20.1 (19.0)	20.5 (19.5)	13.9 (4.3)	7.4 (−4.6)	8.9 (0.3)	13.0 (2.0)
	Avg	20.2	20.6	17.5	10.6	17.3	17.2
RH [%]	Max	63.1	100.0	90.1	87.6	87.9	90.5
Year 2 (T2)		(77.5)		(100.0)	(100.0)	(100.0)	(100.0)
	Min	60.1 (41.5)	100.0	52.9 (16.0)	54.7 (4.0)	42.0 (11.0)	63.5 (28.5)
	Avg	61.8	100.0	74.4	72.8	67.1	78.6
Temp [°C]	Max	20.1 (22.0)	21.0 (22.0)	22.8 (40.7)	13.2 (29.5)	22.8 (41.4)	16.9 (31.1)
Year 3 (T3)	Min	19.8 (17.0)	20.2 (19.6)	13.5 (1.4)	4.0 (−6.4)	11.4 (−4.1)	9.1 (−1.1)
	Avg	19.9	20.3	17.3	9.7	17.1	13.0
RH [%]	Max	63.9	100.0	87.9	86.0	86.2	93.0
Year 3 (T3)		(77.5)		(100.0)	(100.0)	(100.0)	(99.0)
	Min	61.7 (43.0)	100.0	48.8 (16.0)	50.5 (6.0)	45.6 (9.0)	61.5 (23.0)
	Avg	62.9	100.0	70.7	71.3	66.5	79.4
Temp [°C]	Max	20.5 (23.0)	20.2 (20.3)	–	20.7 (31.1)	25.5 (46.0)	19.9 (34.0)
Year 4 (T4)	Min	20.1 (17.0)	20.3 (19.5)	–	12.7 (2.0)	13.9 (2.0)	11.1 (2.0)
	Avg	20.3	20.4	–	16.5	19.3	15.1
RH [%]	Max	62.8	100.0	–	83.3	84.9	88.7
Year 4 (T4)		(77.5)			(100.0)	(88.5)	(100.0)
	Min	57.8 (47.0)	100.0	–	50.9 (4.0)	40.3 (10.0)	59.8 (22.0)
	Avg	60.0	100.0	–	67.2	63.4	76.1

Notes: RH: Relative humidity; Temp: Temperature; Max/Min/Avg: yearly maximum/minimum/average value; the value in parentheses stands for the annual peak value.

carbonation depth.

2.3.2. Epoxy adhesive and CFRP laminate

Tensile tests of both epoxy adhesives and CFRP laminates were performed using MTS UTS machine (Fig. 5a). A total of 125 epoxy adhesive specimens (series of at least 5 specimens for each environment) were tested according to EN ISO 527–2:2012 [46] as shown in Fig. 5b and the elastic modulus was determined according to EN ISO 527–2:2012 [46] by calculating the slope of the secant line on the stress–strain curve between 0.05 % and 0.25 % of the strains. On the other hand, a total of 150 CFRP laminate specimens were also tested in the same configuration (Fig. 5c) as that of the adhesives and according to EN ISO 527–5:2009 [47].

2.3.3. NSM CFRP-to-concrete bond

A total of 50 concrete cubes, each with 200 mm, were used to prepare the specimens strengthened according to NSM technique. The concrete cubes were strengthened with CFRP strips, each being strengthened by 2 CFRP laminates with a bond length of 60 mm (Fig. 6a). For that purpose, two opposed faces parallel to the casting direction were used. The bond length adopted aimed at avoiding the CFRP laminate failure and also to be large enough to represent the system and minimize some inevitable effects such as geometric irregularities [8]. Two of these concrete blocks (4 strengthening systems) were tested at the beginning to serve as reference specimens, whereas the remaining ones were exposed to different environments and tested after exposure. A total of 100 pull-out tests were performed.

The test setup is shown in Fig. 6b, from which the main parts can be highlighted: (i) LVDT support fixation (Fig. 6c); (ii) horizontal and vertical movements restraint (Fig. 6d and Fig. 6e); and (iii) LVDT installation (Fig. 6e). These tests were conducted on four specimens each year (i.e., from T1 to T4). A servo-controlled equipment was used, with the applied force measured by a load cell with a maximum capacity of 200 kN. The tests were performed under displacement control at the loaded end with a rate of 2 μm/s, using a displacement measured through the LVDT1 (Fig. 6a) placed at the loaded end section as a control variable.

3. Results and discussion

This section presents the results from the different tests performed (as described in Section 2), followed by a comprehensive analysis and discussion. Furthermore, comparative studies are also performed between the results from this work and those from the existing literature to derive and propose the environmental conversion factors.

3.1. Test results from the bond constituent materials

3.1.1. Concrete

Concrete compressive strength (f_{cc}), elastic modulus (E_c), pull-off strength (f_{ct}), and carbonation depth (C_d) for all testing time series (T0-T4) and all studied environments (E1-E6) are plotted in Fig. 7a while average values are shown in Table 3. The results show that f_{ct}

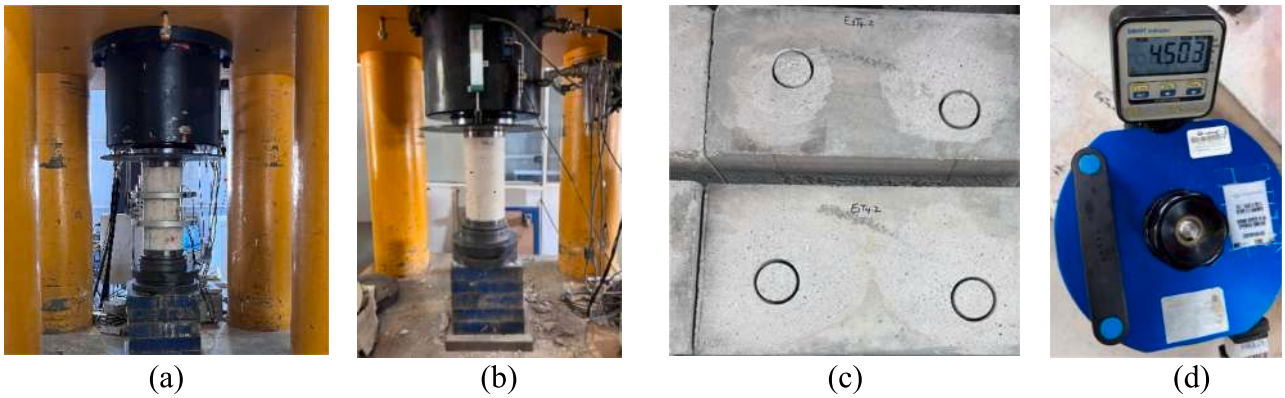

Fig. 4. Tests for concrete characterization: (a) Elastic modulus setup; (b) compression test setup; (c) Sandblasting and creating the cylindrical cores; (d) concrete pull-off test machine.

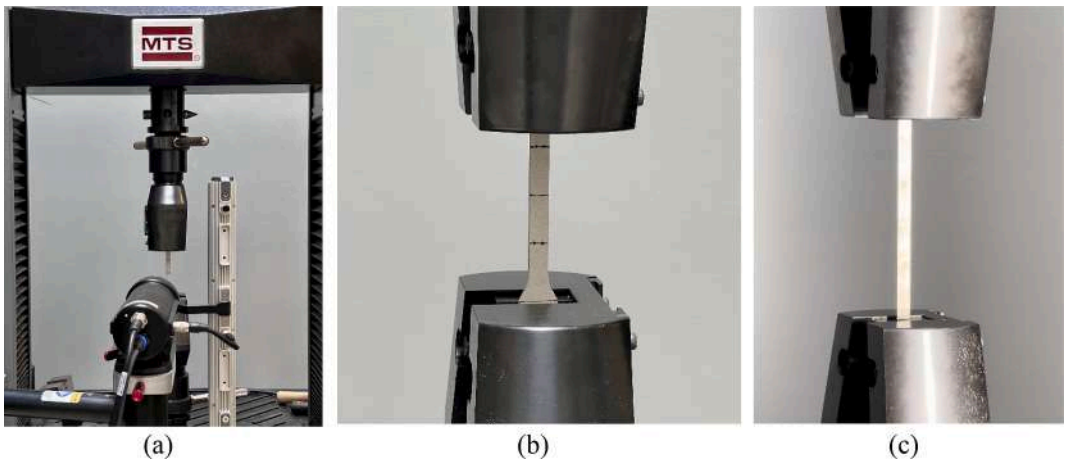

Fig. 5. Tensile tests using a MTS UTS machine: (a) overview of MTS with video extensometer; (b) epoxy adhesive test; (c) CFRP laminate test.

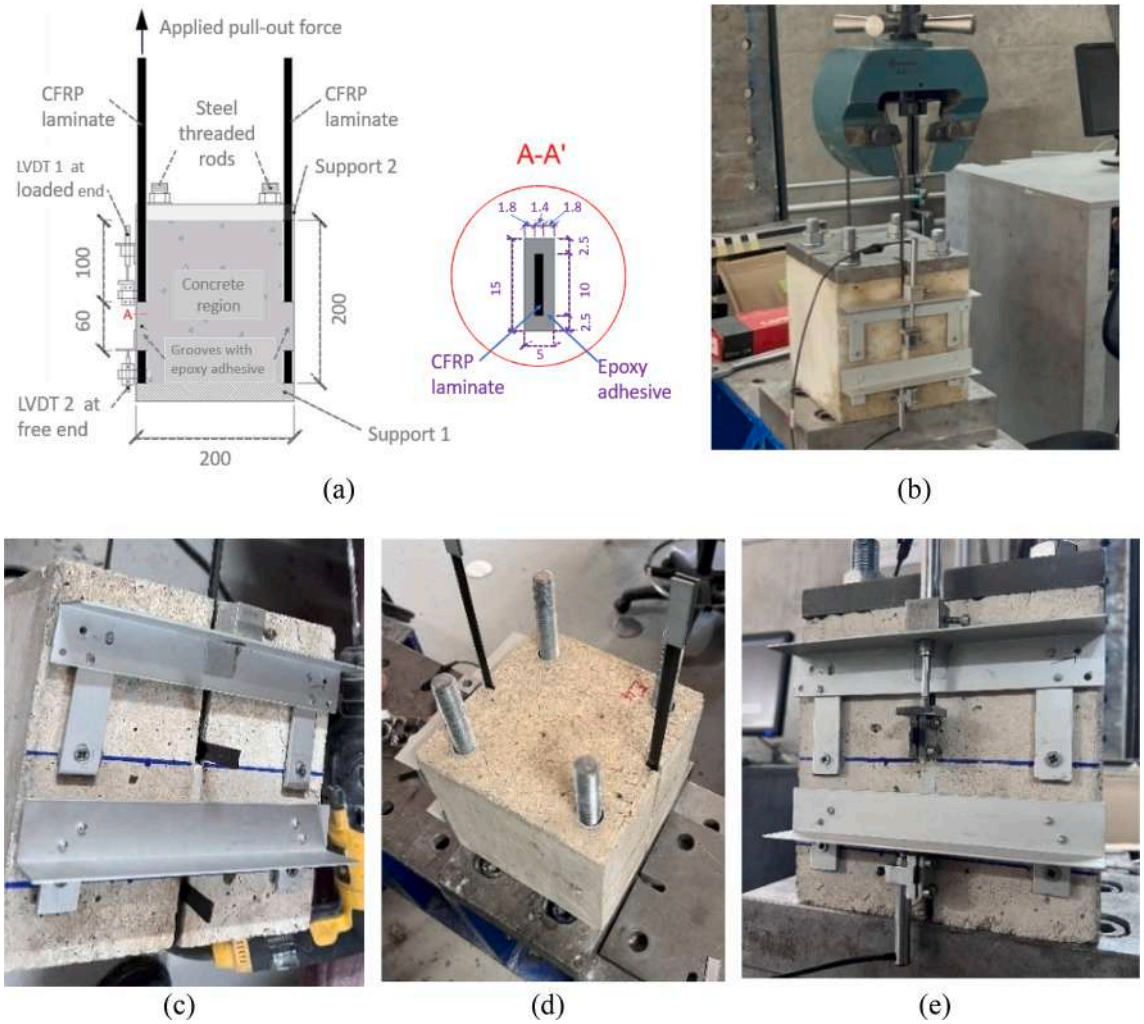

Fig. 6. NSM specimen and single-lap shear test setup: (a) specimen's geometry and test configuration (NSM); (b) photograph of the test; (c) mounting LVDTs supports; (d) installing the specimen; (e) positioning of LVDTs. Note: all units in [mm].

decreased in all studied environments. On the other hand, both f_{cc} and E_c generally improved with time in all outdoor environments. The highest improvements in f_{cc} and E_c were found in E4 and E6 at T2, with increases of 21.2 % and 12.0 % in E4, and 20.9 % and 12.0 % in E6, respectively. The observed increase of f_{cc} and E_c in different environments can be attributed to different factors such as carbonation, temperature variations and continuation of cement hydration. In fact, the C_d is observed to increase linearly with time in E1 (Fig. 7a) due to the relative humidity range [45–77 % RH], see Fig. 3, which is already known to favor the ingress of CO_2 [48].

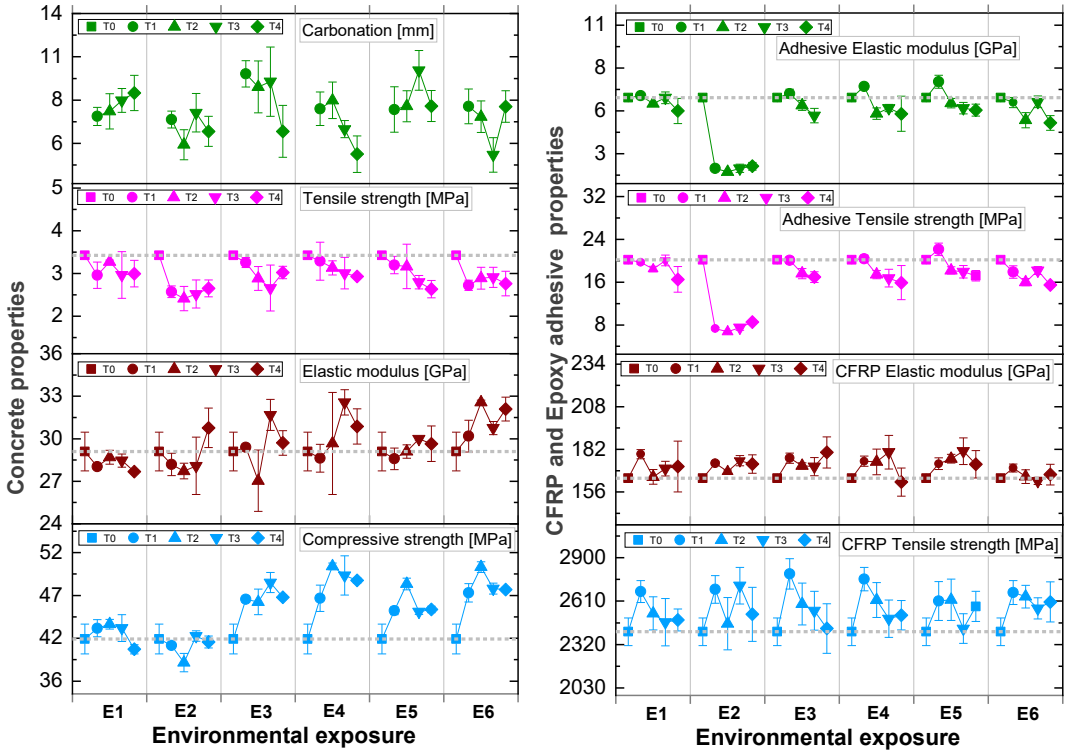

Fig. 7. Variation of material properties under different environments from 0 to 4 years of exposure: (a) concrete, and (b) epoxy adhesive and CFRP laminate.

Table 3
Average values of concrete compressive strength, elastic modulus, pull-off strength, and carbonation depth after 0 (T0), 1 (T1), 2 (T2), 3 (T3), and 4 (T4) years of different environmental exposures (E1 to E6).

Environment	T0	T1	T2	T3	T4	T0	T1	T2	T3	T4
	Compressive strength f_{cc} [MPa]					**Elastic modulus E_c [GPa]**				
REF	41.5 (4.4)	–-	–-	–-	–-	–-	–-	–-	–-	–-
E1	–-	42.8 (2.4)	43.3 (1.4)	42.8 (3.8)	40.3 (1.4)	29.1 (5.0)	28.0 (0.7)	28.7 (1.7)	28.5 (1.6)	27.7 (0.4)
E2	–-	40.7 (0.7)	38.7 (2.9)	41.9 (1.5)	41.1 (1.8)	–-	28.2 (2.8)	27.7 (2.0)	28.1 (7.2)	30.8 (4.5)
E3	–-	46.3 (0.9)	46.0 (3.4)	48.4 (2.5)	46.6 (0.6)	–-	29.4 (0.8)	27.0 (8.0)	31.7 (3.4)	29.7 (2.9)
E4	–-	46.5 (3.4)	50.3 (0.8)	49.2 (4.8)	48.6 (0.7)	–-	28.6 (3.4)	29.7 (12.1)	32.6 (2.7)	30.9 (4.0)
E5	–-	44.9 (1.0)	48.2 (1.5)	44.8 (0.7)	45.1 (0.9)	–-	28.6 (2.6)	29.1 (1.6)	30.0 (0.3)	29.6 (4.2)
E6	–-	47.1 (2.4)	50.2 (1.3)	47.6 (1.4)	47.5 (0.5)	–-	30.2 (3.7)	32.6 (0.5)	30.8 (1.5)	32.1 (2.6)
	Pull-off strength f_{ct} [MPa]					**Carbonation depth C_d [mm]**				
REF	3.4 (13.3)	–-	–-	–-	–-	0.0	–-	–-	–-	–-
E1	–-	2.9 (10.4)	3.2 (1.3)	2.9 (18.4)	2.9 (10.5)	–-	7.4 (19.9)	7.7 (14.8)	8.4 (9.2)	8.9 (12.8)
E2	–-	2.5 (5.3)	2.3 (11.8)	2.5 (13.1)	2.6 (7.4)	–-	7.2 (15.2)	5.5 (17.7)	7.6 (16.4)	6.4 (15.3)
E3	–-	3.2 (3.6)	2.8 (9.7)	2.6 (20.1)	3.0 (4.7)	–-	10.1 (5.5)	9.3 (18.2)	9.6 (23.4)	9.0 (18.8)
E4	–-	3.2 (13.5)	3.1 (5.3)	2.9 (12.2)	2.9 (0.1)	–-	7.8 (7.5)	8.4 (14.1)	6.5 (8.4)	4.9 (24.1)
E5	–-	3.1 (6.3)	3.1 (16.4)	2.7 (5.7)	2.6 (7.7)	–-	7.8 (10.9)	8.0 (12.5)	10.3 (12.4)	8.0 (12.5)
E6	–-	2.7 (4.4)	2.8 (8.8)	2.9 (8.1)	2.7 (10.5)	–-	8.0 (14.1)	7.3 (13.9)	4.9 (22.9)	8.0 (12.8)

Notes: all values in parentheses express coefficient of variation; REF: Reference values from the specimens tested before exposure (i.e., at T0).

However, trends with lower C_d values can be observed from E2 and E4 probably due to increased humidity and moisture in these two environments. This agrees well with the findings by [49] who reported that the increased humidity, rain, and snow slowed down the ingress of CO_2 after exposing concrete to outdoor environments for up to 4 years. Most importantly, the specimens in E2 and E4 are generally found to be partially carbonated (Fig. 8a). Partial carbonation has negligible effects on the concrete properties [50,51] for high relative humidity environments, hence the effects of carbonation in E2 and E4 on the f_{cc} and E_c are negligible. The highest C_d is observed in E3 as expected although there is a surprising decrease in the last year T4 that may be due to climate change issues. Besides, even in other outdoor environments (E5, E6) the C_d is observed to be comparable to that in E3, which may reflect the effects of climate change that causes the abundance of CO_2 in the atmosphere. On the other hand, the observed increase in f_{cc} and E_c in E6 may be further attributed to the synergistic effect between carbonation and chlorides as previously reported in [21].

Studies also show that high temperatures can make concrete more porous thereby increasing the CO_2 penetration [13,14], which may be the reason for the high C_d observed in E5. Hence, the presence of carbonation in E3, E5, E6 can be considered as one of the possible factors that increased the concrete f_{cc} and E_c. This is in line with other previous studies where carbonation was found to increase the f_{cc} [18] and both the f_{cc} and E_c [19]. On the other hand, as previously described for outdoor environments, high temperatures with low RH were recorded in E3 and E5, so this may also have played a major role in increasing the f_{cc} and E_c. This is in agreement with a study by [52], where high temperature variations increased the f_{cc}. Hence, it can be noted that there is a synergistic effect between high temperatures and carbonation, but high temperatures may have played a greater role than the presence of carbonation due to the inconsistent trend of the latter, as shown in Fig. 7a. Contrary, the effects of temperatures on the increase in the f_{cc} and E_c may be thought negligible in E4 and E6 as these environments experienced lower temperature values, hence other factors may have contributed to the observed increased concrete properties.

For example, as a result of the high RH in E4 and E6, continued hydration of cement may occur over time, with the increase of the number of C-S-H silicates, which then occupy the empty voids and push out the diffused moisture in the voids, thereby reducing the porosity and improving concrete properties. Increase of the C-S-H silicates is already known to improve the f_{cc} [53,54]. Increased curing moisture has also been linked to increase in the f_{cc} and E_c [19].

To summarize, the above results show that the increase in concrete properties can result from a combination of more than one factor. In fact, these can be the leading factors in each environment: (i) carbonation in E1; (ii) the competing mechanisms between the increased porosity *versus* cement hydration in E2; (iii) the synergistic effect between carbonation and high temperatures in E3, (iv) the synergistic effect between the continuation of cement hydration and increased humidity in E4; (v) the synergistic effect between high temperatures and carbonation in E5; and, (vi) the synergistic effect of carbonation and chlorides and continuation of cement hydration in E6. Furthermore, comparing the degradation agents, the presence of cement hydration resulting from high relative humidity regions leads to the highest improvement in the concrete f_{cc} and E_c.

The typical failure modes from concrete compression and tensile tests are shown in Fig. 8b, Fig. 8c and Fig. 8d, respectively. In particular, it can be seen that the failure mode from tensile tests occurs deep inside the concrete, as mentioned earlier, which can lead to misleading values since the inner region is ideally not exposed. Finally, the duration and

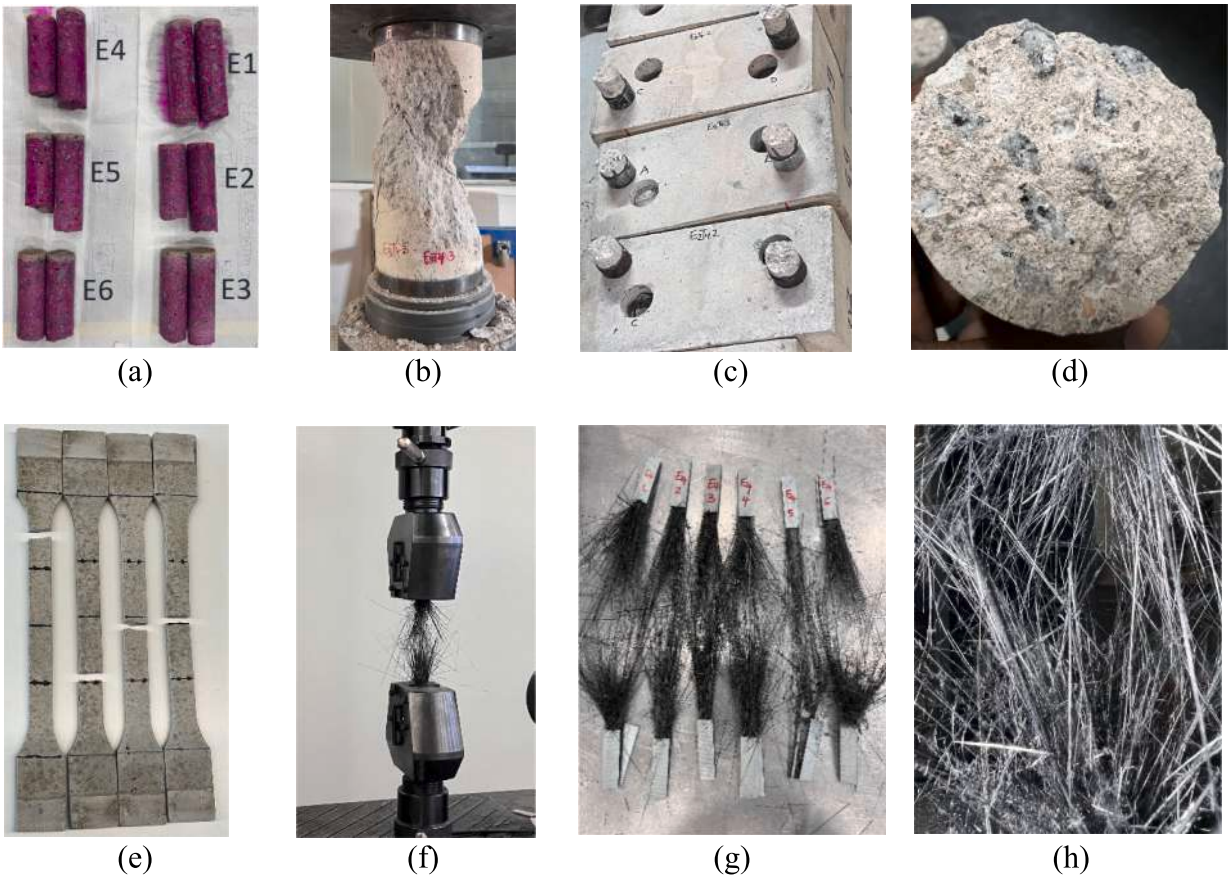

Fig. 8. (a) Carbonation of concrete; typical failure modes from: (b) concrete under compression; (c,d) concrete under tension (pull-off tests); (e) epoxy adhesive under tension; and, (f to h) CFRP laminate under tension.

severity of exposure may have a greater impact on the carbonation depth and elastic modulus of the concrete compared to other properties, due to significant fluctuations rather than a gradual increase or decrease over time. It is possible that the exposure duration was shorter or longer in year i than in year i-1 (for i = 0,…,4), which could have caused these fluctuations. Similarly, fluctuations may also result from differences in exposure severity (i.e., more severe exposures in year i can be thought to lead to higher changes in the properties than in year i-1).

3.1.2. Epoxy adhesive

The average values of the tensile strength (f_a), average elastic modulus (E_a), and ultimate tensile strain (%) of the epoxy adhesive for all testing times and all environments are shown in Fig. 7b, their values in Table 4, and their failure modes in Fig. 8e.

The increase in E_a from T0 to T1 in E1, E3, E4, and E5, is mainly due to the post-curing phenomenon. However, there was a significant decrease in the E_a in E2 which can be attributed to the plasticization effect, and a slight decrease in E6 due to moisture, as the effects of chlorides on the adhesive properties are negligible [27]. Furthermore, a general decrease in the E_a can be observed during the following consecutive years, except for E2 that showed marginal variations after T1. The adhesive f_a shows a similar trend as that of the E_a; however, the effects of the post-curing phenomenon are more pronounced for the latter. The highest decreases in E_a and f_a are found from the specimens immersed in water (E2), with reductions of 75.4 % (at T2) and 66.3 % (at T2), respectively, compared to the value recorded at the initial stage (T0). The reasons for the observed decrease in both the E_a and f_a may be as follows: (i) marginal variations in E1 are due to the effects of increased carbonation, which tends to cause the epoxy resin to cure faster as previously observed in [26], (ii) negative effects of water ingress in E2 and moisture effects in both E4 and E6, which were also found by [11,23], also, in a study by [24], where both the adhesive E_a and f_a decreased due to exposure to wet-dry cycles (case of E4), (iii) in E3, temperatures higher than *Tg* and UV (ultra-violet) radiation can be considered as the main factors that deteriorated the properties of the epoxy adhesive. The failure mode (Fig. 8e) of the adhesive was always an abrupt break in the testing zone of constant cross-section.

Table 4
Average values of CFRP and epoxy adhesives' tensile strength, elastic modulus, tensile strain after 0 (T0), 1 (T1), 2 (T2), 3 (T3), and 4 (T4) years of different environmental exposures (E1 to E6).

Environment	T0	T1	T2	T3	T4	T0	T1	T2	T3	T4
	Adhesive: Tensile strength f_a [MPa]					**CFRP laminate: Tensile strength f_f [MPa]**				
REF	19.9 (3.0)	–-	–-	–-	–-	2405 (3.8)	–-	–-	–-	–-
E1	–-	19.5 (1.8)	18.2 (2.8)	19.8 (4.9)	16.3 (14.6)	–-	2674 (2.72)	2528 (4.4)	2469 (6.4)	2484 (3.0)
E2	–-	7.2 (3.1)	6.7 (2.7)	7.4 (7.1)	8.4 (3.6)	–-	2688 (3.4)	2460 (7.1)	2713 (4.5)	2522 (7.1)
E3	–-	19.9 (3.1)	17.4 (5.3)	16.7 (5.9)	–-	–-	2792 (3.7)	2590 (5.4)	2546 (5.1)	2427 (6.8)
E4	–-	20.1 (3.4)	17.2 (4.3)	16.5 (9.8)	15.7 (20.1)	–-	2757 (2.9)	2617 (4.5)	2492 (5.0)	2516 (3.9)
E5	–-	21.9 (5.2)	18.0 (3.6)	17.7 (6.5)	17.0 (5.8)	–-	2611 (5.0)	2619 (5.3)	2427 (4.1)	2575 (3.9)
E6	–-	17.7 (6.4)	15.8 (4.3)	18.0 (4.2)	15.3 (2.6)	–-	2667 (3.0)	2640 (2.9)	2561 (2.8)	2605 (5.1)
	Adhesive: Elastic modulus E_a [GPa]					**CFRP laminate: Elastic modulus E_f [GPa]**				
REF	6.5 (3.0)					164 (1.2)				
E1	–-	6.6 (1.3)	6.1 (1.4)	6.5 (6.0)	5.6 (14.6)	–-	179 (1.6)	165 (2.7)	170 (2.7)	172 (9.1)
E2	–-	1.9 (5.1)	1.6 (4.0)	1.9 (14.6)	2.0 (12.4)	–-	174 (0.7)	168 (0.6)	175 (1.8)	173 (3.2)
E3	–-	6.7 (4.4)	6.0 (5.4)	5.3 (8.9)	–-	–-	177 (1.8)	172 (1.1)	171(3.3)	180(5.3)
E4	–-	7.2 (1.4)	5.4 (6.9)	5.8 (4.0)	5.4 (21.1)	–-	175 (1.8)	174 (4.5)	180 (5.7)	162 (5.3)
E5	–-	7.5 (5.7)	6.1 (5.0)	5.8 (6.5)	5.7 (7.0)	–-	173 (2.0)	176 (1.5)	181 (4.5)	173 (4.8)
E6	–-	6.2 (5.4)	5.0 (10.0)	6.2 (6.2)	4.8 (10.0)	–-	171 (1.4)	165 (2.5)	163 (2.8)	167 (5.0)
	Adhesive: Ultimate tensile strain [%]					**CFRP laminate: Ultimate tensile strain [%]**				
REF	0.4 (6.2)	–-	–-	–-	–-	14.6 (3.8)	–-	–-	–-	–-
E1	–-	0.4 (13.0)	0.3 (11.7)	0.3 (8.8)	0.4 (11.3)	–-	14.9 (3.2)	15.3 (6.1)	14.5 (7.3)	14.8 (5.3)
E2	–-	1.1 (21.4)	1.1 (11.9)	1.0 (25.5)	0.9 (15.3)	–-	15.5 (2.9)	16.0 (12.5)	15.5 (6.1)	14.9 (1.3)
E3	–-	0.3 (11.1)	0.3 (19.1)	0.3 (10.1)	–-	–-	15.8 (3.8)	15.1 (5.1)	14.6 (8.1)	14.3 (7.0)
E4	–-	0.3 (11.3)	0.3 (12.8)	0.3 (24.6)	0.3 (24.8)	–-	15.78 (2.3)	15.0 (4.5)	13.8 (4.3)	15.4 (1.1)
E5	–-	0.3 (11.2)	0.4 (13.1)	0.3 (11.5)	0.4 (10.5)	–-	15.1 (4.6)	14.9 (2.5)	13.5 (7.0)	15.4 (3.1)
E6	–-	0.3 (4.3)	0.3 (12.9)	0.3 (17.4)	0.4 (14.2)	–-	15.6 (2.9)	16.0 (1.9)	15.7 (2.8)	15.9 (5.0)

Note: all values in parentheses express coefficient of variation in percent; REF: Reference values from the specimens tested at the beginning (before exposure) i.e., at T0.

3.1.3. CFRP laminate

The average values of the tensile strength (f_f), average elastic modulus (E_f), and ultimate tensile strain (%) of the CFRP laminate, for all testing times and all environments are shown in Fig. 7b, their values in Table 4, and their failure modes in Fig. 8f to Fig. 8h.

The CFRP laminate increased both its elastic modulus (E_f) and tensile strength (f_f) as compared to the initial value at T0 (Fig. 7b) and Table 4. This is consistent with the existing literature under AAT where it was reported that CFRP is generally not affected by environmental exposure [11]. The highest increase is generally found at T1, which reflects the effects of post-curing of the fiber resin matrix, followed by a general decrease in subsequent years, but still with higher values than those at T0, except for E5 where the post-curing phenomenon can be expected to still improve both E_f and f_f after 4 years of exposure. The highest values of E_f are found for the specimens in E5 with 10.4 % (at T3) and in E3 with 9.8 % (at T4) increases, while the highest values of the f_f are found in E3 with 16.1 % (at T1) and E4 with 14.6 % (at T1) increases, compared to the value recorded at the initial stage (at T0).

The improved CFRP properties in E1 and E2 during the first year of exposure may be due to the effects of post-curing of the polymeric matrix resin, also observed in [26]. In the following years, reductions on the mechanical properties were observed in both environments: while for the case of E2 the decrease can be supported by water diffusion through the polymeric matrix of the CFRP laminates (physical and chemical aging), for environment E1 no apparent reason could be found. In E3, both carbonation and high temperatures may also lead to a significant post-curing effect of the resin matrix, while in E4 post-curing may be the reason for the observed increased values and the matrix microcracking due to freeze-thaws cycles may be assumed to be the main reason for the slight decrease observed later, as freeze–thaw cycling are known to lead

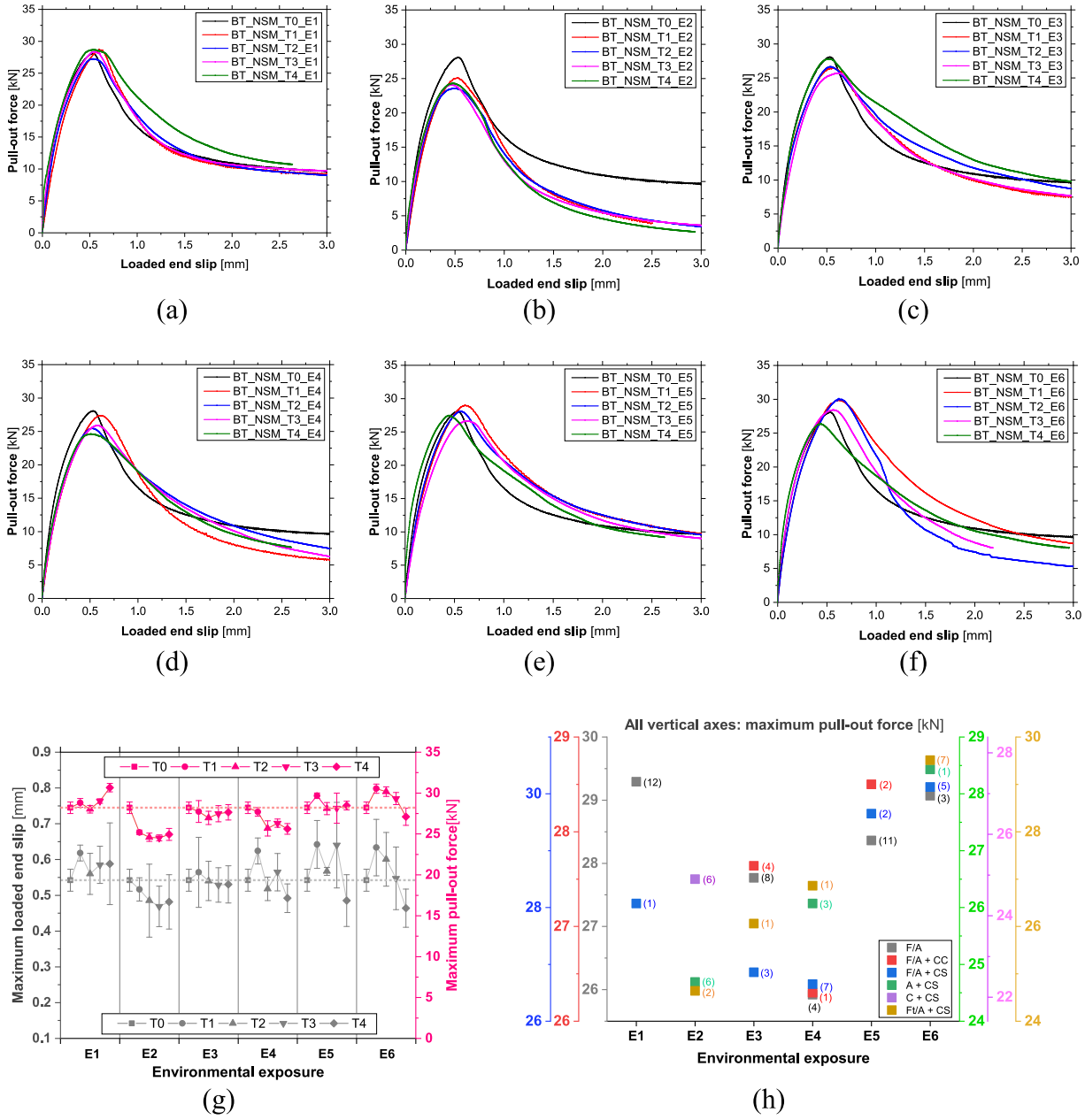

Fig. 9. NSM CFRP-to-concrete bond test results: (a-f) average curves of the loaded end slip *vs* pull-out force for all testing times and all studied environmental exposures; (g) comparison of maximum pull-out force and loaded end slip trends; (h) types of failure modes and their corresponding maximum pull-out forces (numbers in parentheses indicate the number of specimens failed with the shown failure mode, the images of the typical failure mode are shown in Fig. 10 and the legend of Fig. 9h is explained in the caption of Fig. 10).

to microcracks of the polymeric matrix thereby decreasing the material property [29]. In E5, a synergistic effect between high temperatures and the presence of carbonation can be attributed to the observed increased CFRP properties.

Furthermore, in E6 only post-curing and carbonation can be inferred to be the underlying reason for the increased CFRP properties, mainly because chlorides do not affect the CFRP properties according to [11]. The failure modes were characterized by a rapid and progressive fracture of individual fibers starting from the edges and moving towards the center of the CFRP until complete fiber rupture (Fig. 8g and Fig. 8h) with a massive sound.

Overall, a general observation from the bond constituent materials is that the adhesive showed significant degradation, while concrete and CFRP laminate improved their properties after exposure to most environments (except concrete in E2).

3.2. NSM CFRP-to-concrete bond

This section presents the data from the single-lap shear tests performed on the specimens strengthened according to NSM technique. The average pull-out force *versus* loaded end slip curves, their maximum values and their variations are shown in Fig. 9a to Fig. 9f and Table 5. Additionally, the maximum pull-out force (F_{max}) and the loaded end slip at the F_{max}, and the pull-out force *versus* loaded end slip curves for all tested specimens are shown in the Annex I and Annex II, respectively. Furthermore, the variations of both the maximum pull-out force and slip compared to the values at initial time (T0) are presented in Table 6. Comparative plots of the maximum pull-out force and loaded end slip at F_{max}, the observed failure modes with their corresponding F_{max}, and the typical observed failure mode are shown in Fig. 9g, Fig. 9h, and Fig. 10, respectively.

Fig. 9a to Fig. 9f shows an initial linear branch at smaller values of slip, followed by a nonlinear branch up to the peak load at larger slip values. Thereafter, starting from the peak, a descending branch develops as a result of the decay of the pull-out force. Similar trends were also found by [7] and [8]. After the peak, within the descending branch, the pull-out force decrease can be due to several factors depending on the failure mode. It can be inferred that when the failure mode is by concrete cohesive failure (CC), the behavior is closely related to the friction of aggregates and cement paste, while when the failure mode is by adhesive failure (F/A), the dominant factor is the frictional forces between adhesive and CFRP. A visual examination during the test showed that the cracks first appeared in the region near the loaded end section and gradually moved toward the free end region as the applied load increased, which also demonstrates that the maximum shear stresses moved from the loaded end to the free end region as the load increased. This is in good agreement with the examination performed using digital image correlation (DIC) in [7].

From Table 6, it can be seen that the pull-out force decreased in E2, E3, and E4 for all test times (T1 to T4) as compared to the initial values at T0. The largest reductions were obtained for the specimens immersed in water (E2), followed by those of E4, indicating that the NSM CFRP-to-concrete bond is significantly affected by water diffusion and freeze–thaw attack. In fact, there was an average reduction of nearly 12 % and 9 % in the pull-out forces from E2 and E4, respectively, considering all testing times (T1-T4). Besides, the largest reduction in the slip was also found in E2 with a 13.5 % reduction at T3 and an average of nearly 10 % reduction in E2 considering all testing times. In contrast, specimens in E1 generally showed an increase in the pull-out force with an increase of almost 9 % at T4 and an average of nearly 3 % increase over all test times, compared to T0.

The comparative perspectives between the variation of the pull-out force and the variation of the slip (in various environmental exposures) over time are shown in Fig. 9g. In fact, the pull-out force has different variation trend when compared to that of the slip in E3, E4, and E5, while similar trends can be seen in E1, E2, and E6. Therefore, attempts to establish long-term predictions using the force *vs* slip relationship can be simpler in the latter environments (i.e., E1, E2, and E6) than in the former. However, since the trends from the percentage increase/decrease of the force and slip are not similar (Table 6), they cannot be used to establish such models; hence, the models based on the force-slip relationships may be better than those based on the percentage increase/decrease of the force-slip relationships.

Furthermore, Fig. 9h is used to relate the failure mode (notations used Fig. 9h are defined in Fig. 10) with the maximum pull-out force, and to help predict the predominant failure mode in each environment: (i) the failure at the adhesive-CFRP interface (FA); (ii) adhesive-CFRP interface with debonding at CFRP bondline (Ft/A); (iii) concrete cohesive (C); (iv) concrete cracking (CC); (v) concrete splitting (CS); and, (vi) adhesive cohesive (A). It can be seen that F/A failure is the leading failure mode in E1, E3 and E5, while A + CS and C + CS are the two competing failure modes in E2; F/A + CS dominates in E4, while Ft/A + CS dominates in E6.

It can also be seen that the same failure mode does not result in the same maximum pull-out force when considering different environments. For example, the F/A failure in E4 corresponds to a pull–out force of around 25.8 kN, while the corresponding force in E1 is approximately 29.3 kN. Classifying the dominant failure mode according to environmental exposures and their corresponding pull-out forces can pave the way towards developing appropriate analytical or numerical predictions that take into account the expected failure mode, the expected failure load and the type of environment.

Table 5
Average maximum pull-out force and average loaded end slip of NSM technique for all testing times and all studied environments.

Environment	Fmax [kN]					Loaded slip [mm]				
	T0	T1	T2	T3	T4	T0	T1	T2	T3	T4
E1	28.21	28.81	28.03	29.02	30.67	0.54	0.62	0.56	0.59	0.59
	(2.5)	(1.9)	(1.7)	(0.9)	(1.7)	(28.7)	(3.6)	(10.3)	(8.9)	(19.4)
E2	–-	25.19	24.60	24.52	24.95	–-	0.52	0.49	0.47	0.48
		(1.1)	(2.0)	(1.5)	(2.9)		(6.3)	(21.0)	(12.1)	(15.8)
E3	–-	27.75	26.96	27.49	27.65	–-	0.56	0.54	0.53	0.54
		(4.8)	(3.0)	(3.6)	(3.4)		(17.4)	(8.6)	(8.7)	(9.1)
E4	–-	27.71	25.68	26.32	25.62	–-	0.62	0.52	0.56	0.49
		(1.9)	(3.6)	(1.9)	(2.6)		(5.8)	(6.3)	(9.2)	(8.2)
E5	–-	29.68	28.11	28.15	28.47	–-	0.64	0.57	0.64	0.48
		(1.1)	(2.6)	(6.5)	(1.9)		(10.4)	(1.9)	(18.7)	(14.9)
E6	–-	30.54	30.18	29.33	27.11	–-	0.63	0.60	0.55	0.46
		(1.8)	(4.8)	(2.5)	(3.9)		(12.5)	(12.5)	(16.0)	(11.5)

Note: values in parentheses are coefficient of variation in %.

Table 6
Variation of pull-out force and loaded end slip referring to the initial value at T0 for all studied environments.

Environment	Variation of maximum force with time (%)				Variation of loaded end slip with time (%)			
	T1	T2	T3	T4	T1	T2	T3	T4
E1	(+) 2.13	(−) 0.64	(+) 2.87	(+) 8.72	(+) 14.05	(+) 3.23	(+) 7.91	(+) 8.47
E2	(−) 10.71	(−) 12.80	(−) 13.08	(−) 11.56	(−) 4.75	(−) 10.51	(−) 13.52	(−) 11.14
E3	(−) 1.63	(−) 4.43	(−) 2.55	(−) 1.99	(+) 4.06	(−) 0.37	(−) 2.46	(−) 2.16
E4	(−) 1.77	(−) 8.97	(−) 6.70	(−) 9.18	(+) 15.08	(−) 4.48	(+) 4.14	(−) 9.28
E5	(+) 5.21	(−) 0.35	(−) 0.21	(+) 0.92	(+) 18.45	(+) 4.56	(+) 18.07	(−) 10.50
E6	(+) 8.26	(+) 6.98	(+) 3.97	(−) 3.90	(+) 16.83	(+) 10.76	(+) 0.96	(−) 14.41

Notes: (+): increase in %, (−): decrease in %, E1-E6: studied environments, T1-T4: Exposure time from year 1 (T1) to year 4 (T4).

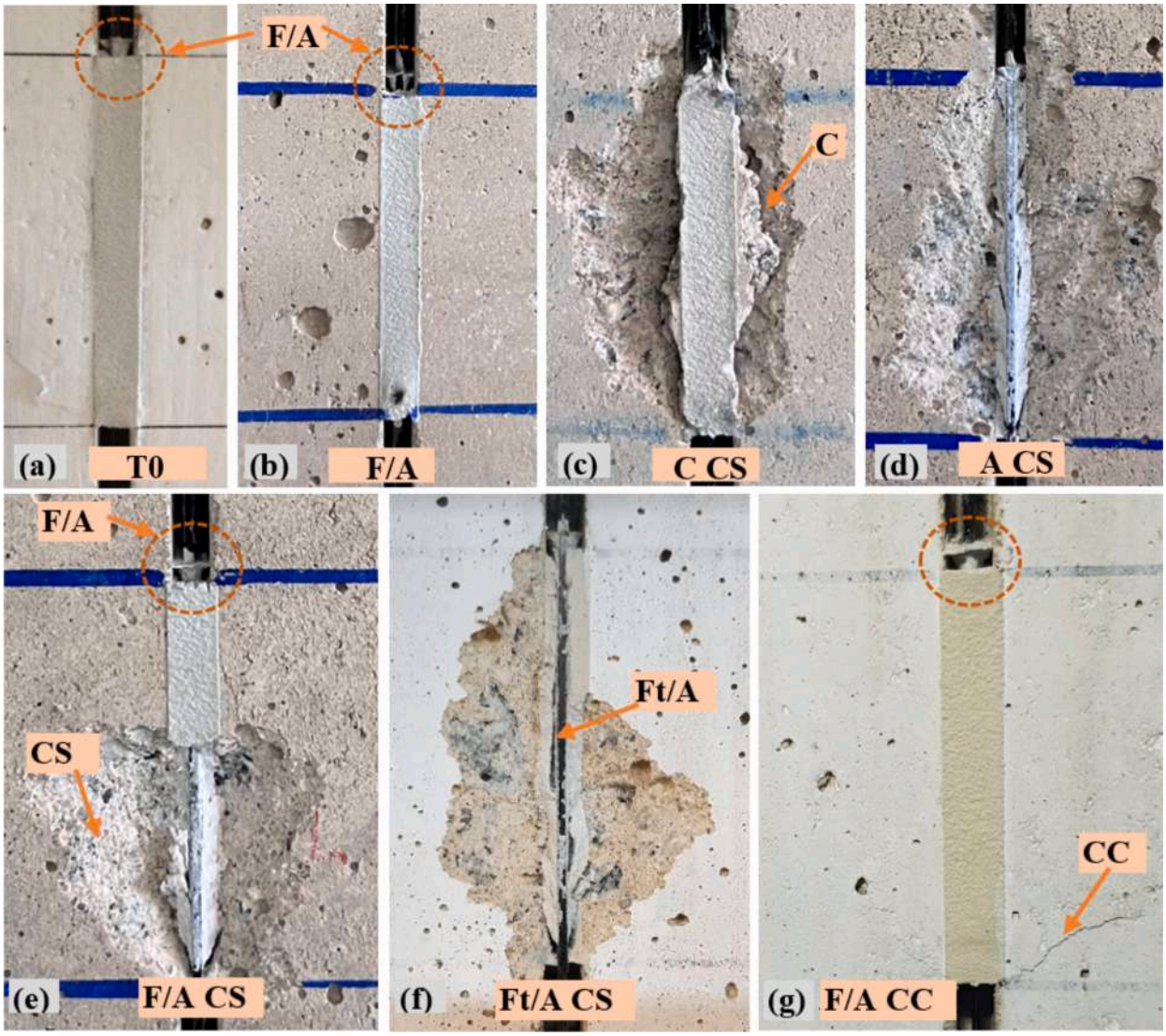

Fig. 10. Typical failure modes observed in the NSM CFRP-to-concrete bond specimens: (a,b) F/A: failure at the adhesive-CFRP interface; (c) C + CS: mixed concrete cohesive and concrete splitting failures; (d) A + CS: mixed adhesive cohesive and concrete splitting failures; (e) F/A + CS: mixed adhesive-CFRP interface and concrete splitting failures; (f) Ft/A + CS: mixed adhesive-CFRP interphase with debonding at CFRP bondline and concrete splitting failures; (g) F/A + CC: mixed adhesive-CFRP interface and concrete cracking failures.

3.3. NSM CFRP-to-concrete bond properties versus constituent materials properties

For a better understanding of the obtained results, presented in Section 3.2, the strength retentions for both the NSM CFRP-to-concrete bond and the bond constituent materials are plotted in Fig. 11a, and the retentions of the bond stiffness and elastic modulus of the bond constituent materials are plotted in Fig. 11b. In the present work, *retention* was defined as the ratio between the actual value of the material property (after exposure) and the original one (before exposure). It is worth noting that the bond stiffness was obtained from the linear fit of the experimental pull-out *vs* loaded end slip curve, considering the range of force from 0 to 10 kN. A detailed analysis of the data obtained here is given in the following paragraphs.

Environment E1: The bond strength generally increases in E1. As previously shown in Section 3.2, both the f_{cc} and f_f generally increased,

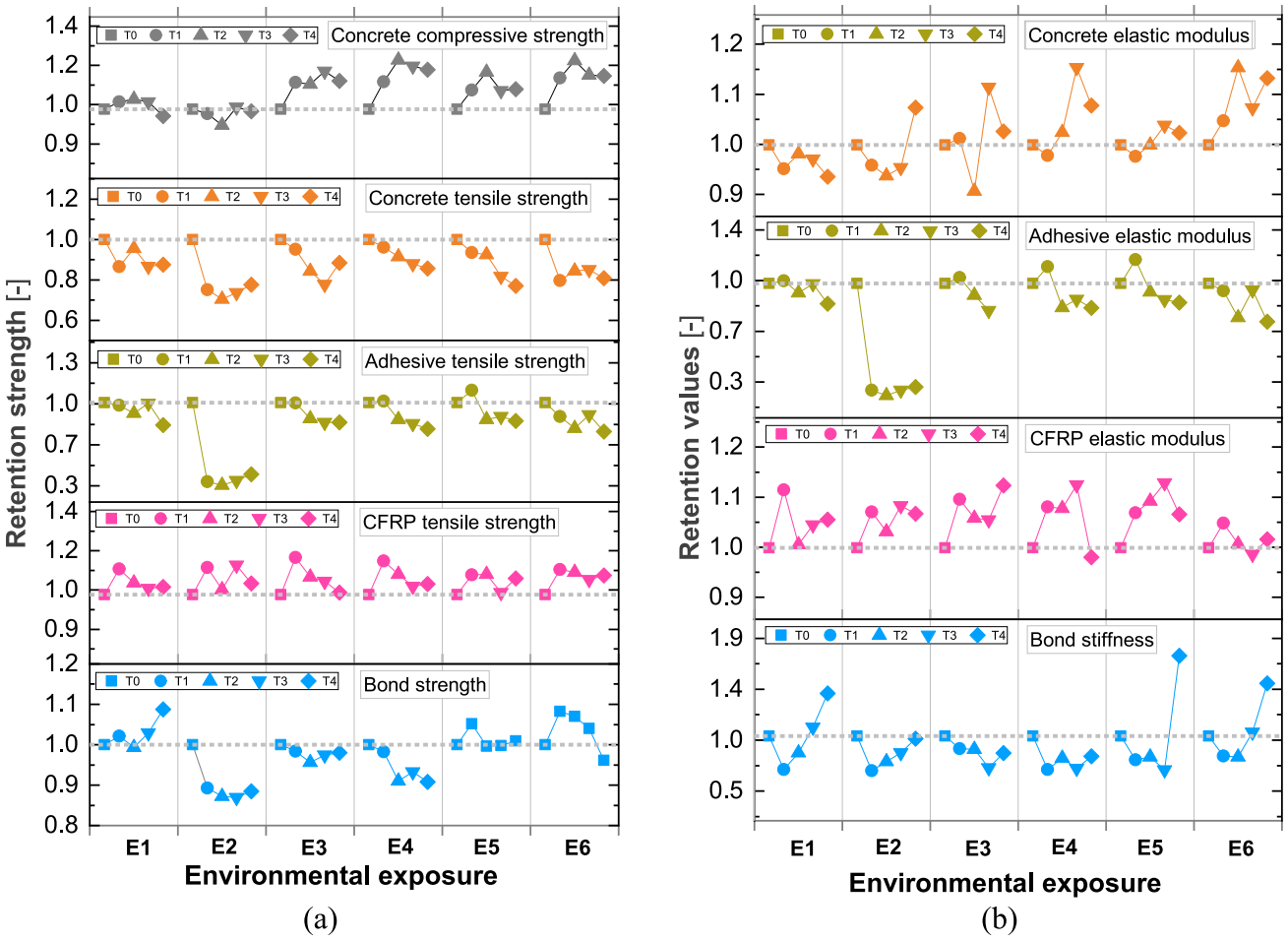

Fig. 11. Variation of properties of bond and its constituent materials: (a) comparative perspectives between the bond strength and material strength properties, (b) comparative perspectives between the bond stiffness and material elastic modulus properties.

while the f_{ct} and f_a slightly decreased, as shown in Fig. 11a. The variations in material properties can cause alteration of the bond properties. That is, the number of bonds (e.g., covalent or hydrogen bonds) linking the epoxy adhesive to the CFRP laminate or those linking the adhesive to concrete augmented, which consequently increased the bond strength (Fig. 11a). On the other hand, the bond stiffness and elastic modulus of the constituent materials are presented in Fig. 11b. The bond stiffness shows a decrease in the first year and a progressive increase in the later years. It can be noted that only the E_c decreased in the first year while the E_a and E_f increased, hence the decreased bond stiffness may be largely due to the E_c degradation. In the later years, the slight reductions in the E_c and E_a may have been outweighed by the increase in E_f, resulting in increased bond stiffness. Overall, it can be concluded that the improvements in f_{cc} and E_c and f_f and E_f outweighed the slight reductions in the f_{ct} and f_a, resulting in increased bond strength and bond stiffness. However, it is worth noting that the bond properties may also be affected by other factors such as the interactive mechanisms taking place at the interface level, rather than the change of the sole properties of the bond constituent materials". Additionally, the materials specimens were fully exposed, while those for pull-out tests were partially exposed (i.e., epoxy adhesive was partially covered by concrete and CFRP laminate, and the CFRP was partially covered by the epoxy adhesive), hence poor correlations between the trends of the variations of the material properties and those of the bond properties are inevitable.

Environment E2: the bond strength decreases sharply from T0 to T1, and then shows marginal decreases until T4. As previously seen, the concrete and adhesive significantly decreased their tensile strength, while a slight decrease in f_{cc} and increase in f_f were observed (in Fig. 11a). Since the bond strength retentions follow the same trend as those of the f_{ct} and f_a, this may be an indicator that the bond strength is strongly dependent on the tensile properties of the concrete and adhesive tensile properties rather than the E_c and E_f properties. The f_{ct} retention (0.7) is comparable to that of the bond strength (0.85), while that of the f_a is much smaller (around 0.3). Hence, both the concrete and adhesive tensile properties degradation can be considered as the main cause of the observed bond strength degradation, with the latter contributing almost 2.5 times more than the former. Besides, E2 is the only environment where specimens showed C + CS and A + CS as the equally dominant failure modes (Fig. 9h), hence analytical models can be established mainly focusing on these two failure modes. On the other hand, the bond stiffness shows a decreasing trend from T0 to T1 and an increasing trend up to T4. The E_c tends to show a similar trend as that of the bond stiffness, while the adhesive shows a different trend. This indicates that the trend of bond stiffness may depend more on E_c and E_f than on E_a. However, since there is a significant loss in the adhesive E_a retention (nearly 0.72 loss at T1) which almost corresponds to a retention of the bond stiffness (of about 0.45), it can be inferred that the decreased adhesive E_a retention may affect the bond stiffness during the water diffusion phase through the adhesive. Then, once the water diffusion is stabilized, the improvement in E_f and E_c may counteract the negative effects caused by the decreased E_a retention, allowing the bond to regain its stiffness over time. The predominant failure mode in E2 also confirms the significant loss of the concrete properties, f_{ct} and E_c (i.e., C + CS failure) and the adhesive properties, f_a and E_a, leading to a complete detachment of the adhesive from the CFRP laminate (i.e., the Ft/A + CS failure).

Environment E3: In E3, the bond strength is found to be nearly stable with time, with minor variations as can be seen in Fig. 11a. This is in good agreement with the findings by [7], where bond strength stability was observed. The f_f shows a progressive decrease after post-curing, but with the last value at T4 still being slightly comparable to that recorded at the beginning. Therefore, it can be thought that the improvement of the concrete f_{cc} counteracted the negative effects of the deterioration of its tensile strength (f_{ct}), and the observed minor reductions in the bond strength may be largely attributed to the deterioration of the f_a, mainly because of the similarity of the trend for both the f_a and the bond strength. Similarly, a significant reduction in the E_a retention (up to 0.3) can be considered as a dominant factor for the observed reduction in bond stiffness, as increased elastic modulus retentions are observed for both concrete and the CFRP. The dominant failure mode in E3 (F/A) may also indicate that the degradation of adhesive properties (f_a and E_a) may be the primary cause of the reduced bond strength and bond stiffness retentions.

Environment E4: bond strength and stiffness generally showed a progressive decrease with exposure time. These decreases are closely related to the observed general decrease in the adhesive f_a and E_a with increasing exposure time (Fig. 11a and Fig. 11b). This is in agreement with the findings of [24], where both f_a and E_a decreased after conditioning the specimens in a wet-dry environment, which reduced the fracture energy at the CFRP-concrete bond interface. The freeze–thaw attack in E4 may have caused a mismatch in the coefficient of thermal expansion (CTE) between the fiber and resin, which thereafter led to microcracking that in turn led to a decrease in the chemical bond strength between adhesive and fiber matrix resin. Such a decrease then caused the failure mode to be mainly F/A + CS (see Fig. 9h). The observed significant increase in f_{cc} can also explain why the dominant failure mode was not CC. In general, both bond strength and bond stiffness seem to depend on the adhesive properties mainly because of the observed similar trends. However, the incresae in f_{cc} over time may have prevented the severe degradation in bond strength observed in the case of E2. In a study by [29] using the AAT protocol, the bond strength first increased and then decreased, which is also the case in E4 from T1 to T2 (increase) and then from T2 to T3 (decrease).

Environment E5: There was a 5.2 % increase in the bond strength at T1 compared to the initial value at T0, followed by a decrease from T1 to T2, which then levelled off until T4 (Fig. 11a). Thus, in general, there were marginal changes in the bond strength. This is in good agreement with a study by [7], where the thermal cycles ranging between 20 °C and 80 °C, imposed on the NSM specimens for a period of 180 days, did not significantly affect the bond strength. The observed sharp increase during T1 may be due to the improvement of f_f and f_{ct}, and the level- off after T1 may be due to the continuation of f_a and f_{ct} degradation. The bond strength showed a similar trend as that of the f_a; hence, it may be a good indicator that the bond strength is significantly dependent on the adhesive tensile strength. On the other hand, the bond stiffness decreased from year to year, except for the last year where a surprising sharp increase can be seen (Fig. 11b). The reason for this sharp increase after 4 years is not clear yet; however, this behavior may be revealed in the future, as the testing campaigns will continue for up to 10 years. The observed stiffness decrease is consistent with the findings of [55], where the FRP-concrete interface stiffness decreased with increasing service temperatures; hence, the high seasonal temperatures in E5 can be considered as the reason for the varying bond stiffness. Besides, the reduced bond stiffness may be attributed to the degradation of the adhesive E_a, as the elastic modulus of the other constituent materials showed increasing trends. The predominant failure mode in E5 is adhesive failure at the CFRP-adhesive interface (F/A), which confirms the weakening of the adhesive bond to CFRP due to its reduced properties. The observed failure is also consistent with the findings in a study by [56], where the increased temperatures changed the failures of NSM specimens from concrete shear failure to F/A.

Environment E6: An opposite trend between bond strength and bond stiffness for specimens in E6 can be seen in Fig. 11a and Fig. 11b. There was a sharp increase in the bond strength during T1, followed by a progressive decrease from year to year until T4. The f_{cc} and f_f increased sharply during T1 and somehow leveled off thereafter. It can be inferred that this increase was due to the high rate of cement hydration and of post-curing of polymeric matrix resin which added more additional bonding to the adhesive, thereby increasing bond strength. In fact, it can be inferred that the above additional bonding served two important purposes: (i) by generating crosslinking that counteracted the negative effects from the f_a and f_{ct} deterioration; and (ii) by supplying additional crosslinking that served the role of increasing the bond strength. However, the continuation of the f_a degradation in the later years led to a progressive decrease in the bond strength, mainly because both f_{cc} and f_f leveled off in those years without any additional bonding being supplied. Besides, the increasing trend in bond stiffness may have been significantly dependent on the increased E_c, since the E_a showed reductions in retentions and CFRP showed insignificant variations. Although both concrete and CFRP laminate are accredited for the observed improved bond properties, the former might have played a more relevant role because of its higher retentions (nearly 1.30 for f_{cc} and 1.18 for E_c) than those of the latter (nearly 1.10 for f_f and 1.08 for E_f). This is mainly supported by the observed failure mode, i.e., a mixed failure with Ft/A + CS is predominant (Fig. 9h), which shows that concrete played a more relevant role in increasing the maximum pull-out force because the main failure was not the concrete cohesive. Therefore, concrete properties can be thought to have played a greater role in controlling both the bond strength and bond stiffness in E6.

Overall, it is important to note that the response of the NSM CFRP-to-concrete bond can be thought to depend not only on the behavior of the constituent materials, but also on the behavior of the interface itself as well as the resisting mechanisms, as was previously observed in [4,57]. In addition, the properties of the solely tested constituent materials may differ from those of the region composing the interface, particularly in the case of the adhesive which is partially exposed as it is mostly covered by concrete, and the CFRP laminate which is completely covered by the adhesive.

3.4. Natural outdoor versus laboratory-controlled environments

In outdoor application of CFRP composites as strengthening systems, the CFRP-to-concrete bond and the bond constituent materials are essentially exposed to an outdoor environment. It is of paramount importance to develop correlations between Accelerated Aging Test (AAT) and Natural Aging Test (NAT) data, as this can lead to appropriate recommendations on the reduction factors for quantifying the effects of different outdoor degradation agents on the durability of the materials. In this context, comparisons were made between the existing AAT data from literature and NAT data from the present work, and some environmental conversion (reduction) factors were derived. For this purpose, a database composed of AAT data from different existing studies [7,31–33] was prepared with the following characteristics:

1. Database comprised of 84 specimens strengthened with CFRP strips according to NSM technique, bond length in the range 100–600 mm, specimens tested either in a direct or beam single-lap shear test configuration; type of environmental exposures being accelerated aging, with degradation agents as freeze–thaw cycles, wet-dry cycles, immersion in salt or tap water, moisture, and temperature cycles;
2. Type of CFRP laminate: pultruded composites with thickness and elastic modulus in the range of 1.3–1.4 mm and 155–176 GPa, respectively;
3. Adhesive of epoxy-based type, with the compressive strength in the range of 25–50 MPa;
4. Exposure time: up to 2 years.

The variation of bond strength retention with exposure time is

presented in Fig. 12a for the results from the above-described AAT database together with those from both the AAT (FRPLongDur-E2) and NAT (FRPLongDur- E3-E6) data of the present work. It can be seen that the retentions of the AAT data from existing studies vary approximately between 0.8 and 1.2, thereby showing a significant dispersion. On the other hand, the retentions from the AAT data of the present work show a marginal variation (between 0.8 and 0.9) with a decreasing trend over time. Besides, the NAT data also show a decreasing trend of the strength retentions with time.

In order to derive the environmental conversion factor (ECF) from both the existing AAT data (from the literature) and the NAT data (from the present work), the percentages of non–conservative estimates (i.e., the percentages for which it is assumed that the estimated test data did not result in conservative values, i.e., values that did not fall within the desired range) are plotted against the estimated environmental conversion factors in Fig. 12b. Considering 10 % of the non-conservative data as the maximum allowable percentage, the ECF of 0.88 and 0.93 can be proposed for the AAT and NAT data, respectively. When comparing these two factors, it can be seen that the existing accelerated aging data tends to overestimate the bond strength degradation rate for up to 4 years; however, NAT data covering longer durations, may help to predict more appropriate factors.

4. Conclusion and recommendations

In this study, the durability of the NSM CFRP-concrete bond was addressed. The durability of the bond was assessed after exposure to two laboratory-controlled environments (i.e., one denoted as E1 with conditioning at around 20 °C/55 %RH and other as E2 with water immersion at 20 °C), and four outdoor environments to mainly promote aging due to carbonation (denoted as E3), freeze–thaw attack (E4), elevated temperatures (E5), and airborne chlorides (E6). Materials (concrete, adhesive and CFRP laminates), as well as NSM CFRP-Concrete bond specimens, were tested before exposure at initial time (T0); and after being exposed to the above-mentioned environments (E1-E6), that is, after one year (T1), two years (T2), three years (T3), and fourth years (T4) of exposure. The key findings are highlighted as follows.

1. Although the environmental exposures were carefully selected to promote mainly a single degradation agent, the effects of multiple degradation agents may have occurred within a single environment. Therefore, synergistic effects on the bond properties may have played an important role in the observed variations, particularly in outdoor environments. In fact, the combined effects of carbonation, moisture, and airborne chlorides were the three-competing agents in E6; carbonation and elevated temperature effects were dominant in E3 and E5, while in E4 the effects of moisture and freeze-thaws dominated.
2. *Constituent materials*: The bond constituent materials showed different variations depending on the environmental exposures:
   i. *Concrete*: the concrete compressive strength (f_{cc}) increased sharply during the first years due to the enhanced continuation of cement hydration and then began to level-off in the later years; however, marginal variations were observed in laboratory-controlled environments. Besides, the concrete elastic modulus (E_c) also showed a general improvement in outdoor and a decrease in laboratory-controlled environments. The highest improvements of the concrete f_{cc} and E_c were found in E3 and E5 with 21.2 % and 21.0 % increase, and in E4 and E6 with 12.0 % increase, respectively. Contrary, the concrete pull-off strength (f_{ct}) showed decreasing trends in all environments);
   ii. *Epoxy adhesive*: the adhesive tensile strength (f_a) and its elastic modulus (E_a) decreased in all environments, but with some improvements in E1, E3, E4, and E5 for the case of E_a during the first year as a result of post-curing. The lowest values of the E_a and f_a were obtained from water immersion, with reductions of 75.4 % and 66.3 %, respectively, as compared to the initial values;
   iii. *CFRP laminate*: the CFRP laminate tensile strength (f_f) and its elastic modulus (E_f) increased as a result of post-curing of the polymeric matrix, which can be attributed to the presence of carbonation in E1, synergistic effect between carbonation and high temperatures in E3, between moisture and freeze–thaw in E4, the synergistic effect between carbonation and high temperatures in E5, and synergistic effects between carbonation, moisture and airborne chlorides in E6. The highest values of E_f were found for the specimens in E5 with 10.4 % (at T3) and in E3 with 9.8 % (at T4), while the highest values of the f_f were found in E3 with 16.1 % (at T1) and E4 with 14.6 % (at T1), as compared to the initial value recorded before exposure (at T0).
3. *NSM CFRP-to-concrete bond*: the bond strength and bond stiffness changed over time and from environment to environment. The highest degradations of the bond strength were observed under continuous water immersion (E2) and freeze–thaw attack (E4), with decreases of nearly 12 % and 9 %, respectively. In contrast, the bond

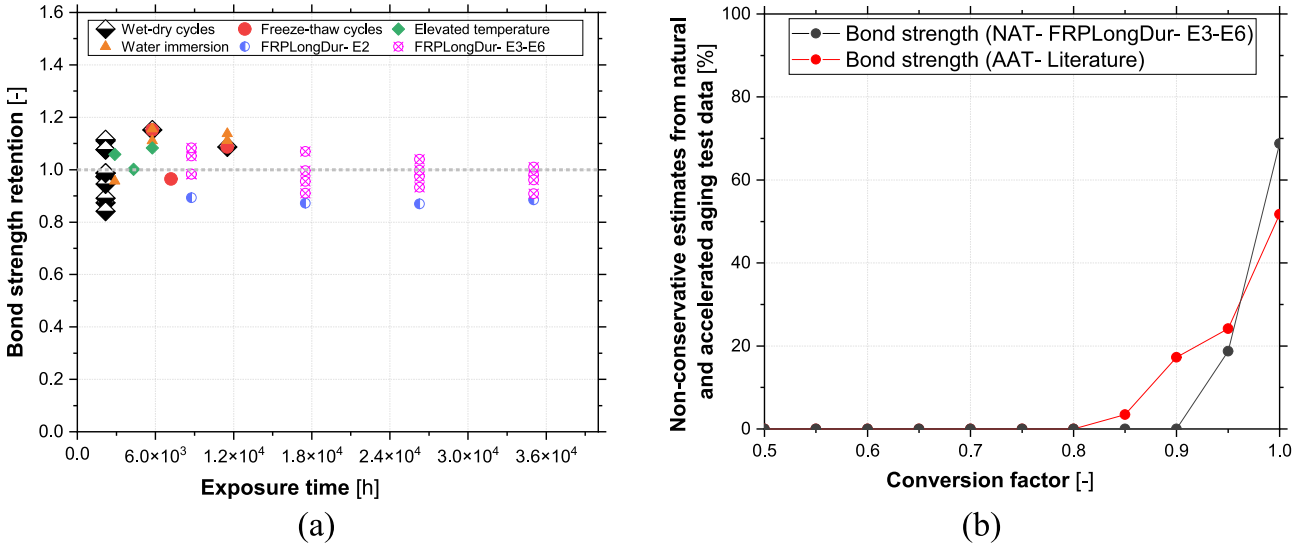

Fig. 12. Comparison of natural *vs*. accelerated ageing durability results for NSM technique: (a) bond strength retention with time for both AAT and NAT; (b) prediction of conversion factors for both AAT and NAT protocols.

strength in E1 generally improved, showing an increase of approximately 10 % in the last year. Similarly, the bond strength in outdoor environments (E5 and E6) generally improved, indicating that exposure to high temperatures (with presence of carbonation) and airborne chlorides (with presence of both carbonation and high humidity) can generally be beneficial to the bond properties in NSM technique. Also, change of concrete properties played a major role in improving bond properties in E6. The effects of atmospheric CO_2 were minimal in E3, with very insignificant changes in the bond strength. On the other hand, the bond stiffness generally showed a decrease (with approximatively 0.7 retentions in all environments) during the first year, followed by a general increase in the following years, remarkable for the specimens in laboratory-controlled environments.

4. *Failure modes*: visual examination of failure modes in NSM showed that the failure mode at initial time (T0) changed after exposure. In general, the failure at adhesive-CFRP interface (F/A) dominated in E1 and E5; the combination of adhesive failure (A) with concrete cohesive failure (CC) or with concrete splitting (CS) dominated in E2; F/A dominated in E3, a combination of F/A and CS dominated in E4 mainly because of the long-lasting negative effects of freeze–thaw on both adhesive and CFRP; F/A or a combination of F/A and CS dominated in E6.
5. The bond strength retentions from the AAT data (from existing studies) vary significantly, ranging approximately between 0.8 and 1.2, which shows a remarkable dispersion. Also, most of AAT bond strength retentions from literature did not agree with those of natural aging test (NAT) from the present work. Attempts were made to derive the ECF. Considering 10 % of the non-conservative estimates from the AAT and NAT data as the maximum allowable percentage, the conversion factors of 0.88 and 0.93 are suggested for the former and the latter, respectively. Comparing these two factors, it can be seen that the existing accelerated aging test data tends to overestimate the bond strength degradation rate for up to 4 years.

As a main recommendation, the authors suggest that studies with NAT data for longer periods (e.g., more than 4 years) of exposure are required to be able to appropriately predict the conversion factors.

CRediT authorship contribution statement

Aloys Dushimimana: Writing – original draft, Methodology, Investigation, Formal analysis, Conceptualization. **José Sena-Cruz:** Writing – review & editing, Validation, Supervision, Project administration, Methodology, Investigation, Funding acquisition. **Luís Correia:** Investigation, Formal analysis, Methodology, Supervision, Validation, Writing – review & editing. **João Miguel Pereira:** Supervision, Validation, Writing – review & editing. **Susana Cabral-Fonseca:** Investigation, Supervision, Validation, Writing – review & editing. **Ricardo Cruz:** Writing – review & editing, Validation, Investigation.

Declaration of competing interest

The authors declare that they have no known competing financial interests or personal relationships that could have appeared to influence the work reported in this paper.

Data availability

Data will be made available on request.

Acknowledgements

This work was carried out in the scope of the project FRPLongDur POCI-01-0145-FEDER-016900 (FCT PTDC/ECM-EST/1282/2014) and DURABLE-FRP (PTDC/ECI-EGC/4609/2020 – DOI 10.54499/PTDC/ECI-EGC/4609/2020) funded by national funds through the Foundation for Science and Technology (FCT) and co-financed by the European Fund of the Regional Development (FEDER) through the Operational Program for Competitiveness and Internationalization (POCI) and the Lisbon Regional Operational Program and, partially financed by the project POCI-01-0145-FEDER-007633 and by FCT/MCTES through national funds (PIDDAC) under the R&D Unit Institute for Sustainability and Innovation in Structural Engineering (ISISE), under reference UIDB/04029/2020 (DOI 10.54499/UIDB/04029/2020), and ARISE under reference LA/P/0112/2020. Furthermore, this work is financed by national funds through FCT under grant agreement DFA/BD/08403/2021 attributed to the first author. The authors also acknowledge all the involved companies: S&P Clever Reinforcement Iberica Lda., Portuguese Institute for Sea and Atmosphere, I.P. (IPMA, IP), Sika Portugal – Produtos Construção e Indústria, S.A., Hilti Portugal – Produtos e Serviços, Lda., Artecanter – Indústria Criativa, Lda., Tecnipor – Gomes&Taveira Lda., Vialam – Indústrias Metalúrgicas e Metalomecânicas, Lda., Laboratório Nacional de Engenharia Civil (LNEC, IP), EDP – Energias de Portugal and APDL, SA.

Annex A.

Single-lap shear test results for all the specimens tested from T0 to T4.

Time	Specimen	F_{lmax} [kN]	s_{lmax} [mm]	F_{lmax} [kN]	s_{lmax} [mm]	F_{lmax} [kN]	s_{lmax} [mm]
T0	No.1	24.47	0.59	–	–	–	–
	No.2	27.55	0.53	–	–	–	–
	No.3	28.81	0.53	–	–	–	–
	No.4	28.99	0.50	–	–	–	–
		E1 E1		**E2 E2**		**E3 E3**	
T1	No.1	28.30	0.65	29.05	0.51	26.98	0.57
	No.2	28.26	0.63	25.53	0.57	29.54	0.71
	No.3	29.16	0.60	24.77	0.49	28.40	0.55
	No.4	29.50	0.60	25.36	0.49	26.06	0.43
T2	No.1	28.07	0.56	24.18	0.42	25.68	0.57
	No.2	28.48	0.63	25.41	0.61	27.11	0.51
	No.3	28.30	0.57	24.62	0.56	27.94	0.48
	No.4	27.27	0.47	24.18	0.35	27.11	0.60
T3	No.1	29.12	0.56	24.11	0.43	28.78	0.64

(*continued on next page*)

(*continued*)

	No.2	28.76	0.63	24.99	0.61	26.28	0.64
	No.3	28.77	0.57	24.20	0.56	26.83	0.40
	No.4	29.43	0.47	24.76	0.47	28.07	0.68
T4	No.1	–	–	25.94	0.59	26.16	0.24
	No.2	30.66	0.63	25.36	0.50	27.70	0.55
	No.3	31.01	0.70	24.30	0.39	28.76	0.44
	No.4	31.18	0.43	24.20	0.44	27.96	0.55
		E4 E4		**E5 E5**		**E6 E6**	
T1	No.1	27.00	0.61	29.29	0.68	30.26	0.59
	No.2	28.28	0.68	29.98	0.60	29.77	0.66
	No.3	27.39	0.63	30.04	0.56	30.96	0.75
	No.4	28.16	0.58	29.39	0.73	31.17	0.54
T2	No.1	26.70	0.54	29.04	0.58	29.90	0.65
	No.2	24.86	0.46	27.01	0.55	27.11	0.47
	No.3	26.50	0.55	27.98	0.58	30.99	0.65
	No.4	24.66	0.52	28.40	0.56	29.65	0.54
T3	No.1	26.86	0.60	28.63	0.82	28.78	0.57
	No.2	26.59	0.65	29.26	0.60	30.11	0.57
	No.3	25.53	0.54	29.66	0.65	28.43	0.41
	No.4	26.30	0.52	25.02	0.49	30.01	0.65
T4	No.1	26.46	0.65	28.36	0.19	28.78	0.57
	No.2	25.68	0.41	27.65	0.41	30.11	0.57
	No.3	24.61	0.44	–	–	28.43	0.41
	No.4	25.73	0.53	28.86	0.54	30.01	0.65

Notes: F_{lmax}: maximum pull-out force; s_{lmax}: loaded end slip at F_{lmax}; E1-E6: studied environments; T0: initial time before exposure; T1-T4: exposure time in years.

Annex B.

Single-lap shear test results: Pull-out force *vs*. loaded end slip curves for all specimens tested up to 4 years.

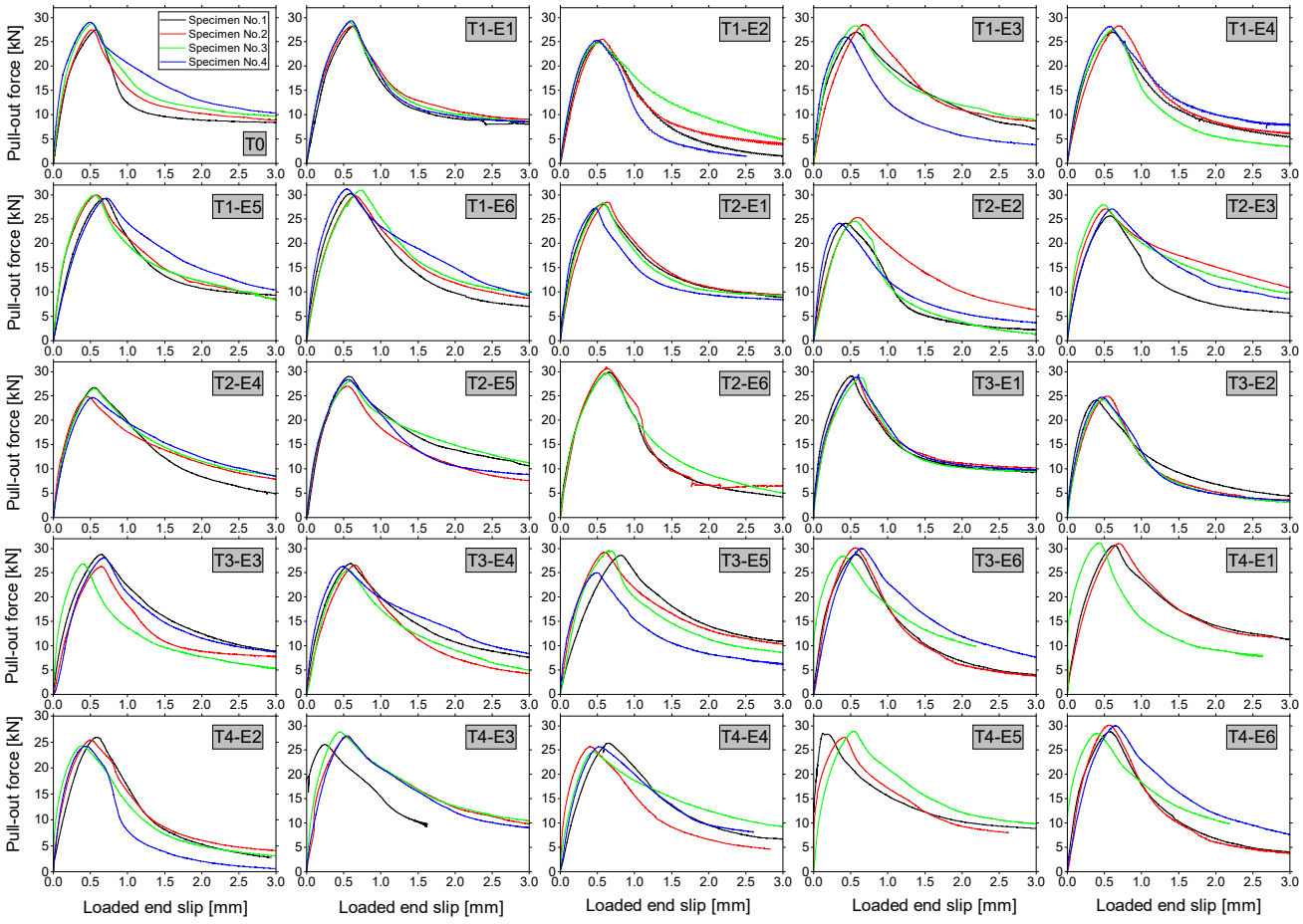

.

References

[1] T. Westphal, P. Bortolotti, R.P.L. Nijssen, Carbon glass hybrid materials for wind turbine rotor blades, 2013. http://resolver.tudelft.nl/uuid:f214ffc8-60c5-4855-a4b9-db3be9991193.

[2] Abbood IS, Odaa SA, Hasan KF, Jasim MA. Properties evaluation of fiber reinforced polymers and their constituent materials used in structures - A review. Mater Today Proc 2021;43:1003–8. https://doi.org/10.1016/j.matpr.2020.07.636.

[3] CEB-FIP, fib90 Bulletin:Externally Applied FRP reinforcement for Concrete structures, 2019.

[4] Cruz JS, Barros J. Modeling of bond between near-surface mounted CFRP laminate strips and concrete. Comput Struct 2004;82:1513–21. https://doi.org/10.1016/j.compstruc.2004.03.047.

[5] De Lorenzis L, Teng JG. Near-surface mounted FRP reinforcement: An emerging technique for strengthening structures. Compos Part B Eng 2007;38:119–43. https://doi.org/10.1016/j.compositesb.2006.08.003.

[6] Coelho MRF, Sena-Cruz JM, Neves LAC. A review on the bond behavior of FRP NSM systems in concrete. Constr Build Mater 2015;93:1157–69. https://doi.org/10.1016/j.conbuildmat.2015.05.010.

[7] Fernandes P, Sena-Cruz J, Xavier J, Silva P, Pereira E, Cruz J. Durability of bond in NSM CFRP-concrete systems under different environmental conditions. Compos Part B Eng 2018;138:19–34. https://doi.org/10.1016/j.compositesb.2017.11.022.

[8] Cruz R, Correia L, Cabral-Fonseca S, Sena-Cruz J. Durability of bond between NSM CFRP strips and concrete under real-time field and laboratory accelerated conditioning. J Compos Constr 2022;26:1–15. https://doi.org/10.1061/(asce)cc.1943-5614.0001262.

[9] Correia L, Teixeira T, Michels J, Almeida JAPP, Sena-Cruz J. Flexural behaviour of RC slabs strengthened with prestressed CFRP strips using different anchorage systems. Compos Part B 2015;81:158–70. https://doi.org/10.1016/j.compositesb.2015.07.011.

[10] El-Hacha R, Wight R, Green M. Prestressed fibre-reinforced polymer laminates for strengthening structures. Prog Struct Eng Mater 2001;3:111–21. https://doi.org/10.1002/pse.76.

[11] Cruz R, Correia L, Dushimimana A, Cabral-Fonseca S, Sena-Cruz J. Durability of epoxy adhesives and carbon fibre reinforced polymer laminates used in strengthening systems: Accelerated ageing versus natural ageing. Materials (Basel) 2021;14. https://doi.org/10.3390/ma14061533.

[12] Tatar J, Brenkus NR. Performance of FRP-strengthened reinforced concrete bridge girders after 12 years of service in coastal florida. J Compos Constr 2021;25. https://doi.org/10.1061/(asce)cc.1943-5614.0001134.

[13] Huang NM, Chang JJ, Liang MT. Effect of plastering on the carbonation of a 35-year-old reinforced concrete building. Constr Build Mater 2012;29:206–14. https://doi.org/10.1016/j.conbuildmat.2011.08.049.

[14] Talakokula V, Bhalla S, Ball RJ, Bowen CR, Pesce GL, Kurchania R, et al. Diagnosis of carbonation induced corrosion initiation and progression in reinforced concrete structures using piezo-impedance transducers. Sensors Actuators, A Phys 2016;242:79–91. https://doi.org/10.1016/j.sna.2016.02.033.

[15] Han Shen X, Feng Liu Q, Hu Z, Qiang Jiang W, Lin X, Hou D, Hao P. Combine ingress of chloride and carbonation in marine-exposed concrete under unsaturated environment: A numerical study. Ocean Eng 2019;189:106350. https://doi.org/10.1016/j.oceaneng.2019.106350.

[16] Medvedev V, Pustovgar A. A review of concrete carbonation and approaches to its research under irradiation. Buildings 2023;13.

[17] Roy SK, Northwood DO, Pohs KB. Effect of plastering on the carbonation of a 19-year-old reinforced concrete building. Constr Build Mater 2012;29:206–14. https://doi.org/10.1016/j.conbuildmat.2011.08.049.

[18] Al Fuhaid AF, Niaz A. Carbonation and corrosion problems in reinforced concrete structures. Buildings 2022;12:1–20. https://doi.org/10.3390/buildings12050586.

[19] Mi Z, Hu Y, Li Q, An Z. Effect of curing humidity on the fracture properties of concrete. Constr Build Mater 2018;169:403–13. https://doi.org/10.1016/j.conbuildmat.2018.03.025.

[20] Zhao J, Cai G, Cui L, Si Larbi A, Tsavdaridis KD. Deterioration of basic properties of the materials in FRP-strengthening RC structures under ultraviolet exposure. Polymers (Basel) 2017;9. https://doi.org/10.3390/polym9090402.

[21] Wang Y, Nanukuttan S, Bai Y, Basheer PAM. Influence of combined carbonation and chloride ingress regimes on rate of ingress and redistribution of chlorides in concretes. Constr Build Mater 2017;140:173–83. https://doi.org/10.1016/j.conbuildmat.2017.02.121.

[22] Kuosa H, Ferreira RM, Holt E, Leivo M, Vesikari E. Effect of coupled deterioration by freeze-thaw, carbonation and chlorides on concrete service life. Cem Concr Compos 2014;47:32–40. https://doi.org/10.1016/j.cemconcomp.2013.10.008.

[23] P. Fernandes, P. Silva, L. Correia, J. Sena-cruz, Durability of an epoxy adhesive and a CFRP laminate under different exposure conditions, in: Third Conf. Smart Monit. Assess. Rehabil. Civ. Struct. 2015, 2015: p. 9.

[24] Cui E, Jiang S, Wang J, Zeng X. Bond behavior of CFRP-concrete bonding interface considering degradation of epoxy primer under wet-dry cycles. Constr Build Mater 2021;292:123286. https://doi.org/10.1016/j.conbuildmat.2021.123286.

[25] Grammatikos SA, Jones RG, Evernden M, Correia JR. Thermal cycling effects on the durability of a pultruded GFRP material for off-shore civil engineering structures. Compos Struct 2016;153:297–310. https://doi.org/10.1016/j.compstruct.2016.05.085.

[26] Dong Hu D, Xun Lyu J, Liu T, Dong Lang M, Zhao L. Solvation effect of CO2 on accelerating the curing reaction process of epoxy resin. Chem Eng Process - Process Intensif 2018;127:159–67. https://doi.org/10.1016/j.cep.2018.01.027.

[27] Silva P, Fernandes P, Sena-Cruz J, Xavier J, Castro F, Soares D, et al. Effects of different environmental conditions on the mechanical characteristics of a structural epoxy. Compos Part B Eng 2016;88:55–63. https://doi.org/10.1016/j.compositesb.2015.10.036.

[28] Liu S, Pan Y, Li H, Xian G. Durability of the bond between CFRP and concrete exposed to thermal cycles. Materials (Basel) 2019;12. https://doi.org/10.3390/ma12030515.

[29] Jiang F, Han X, Wang Y, Wang P, Zhao T, Zhang K. Effect of freeze-thaw cycles on tensile properties of CFRP, bond behavior of CFRP-concrete, and flexural performance of CFRP-strengthened concrete beams. Cold Reg Sci Technol 2022;194:103461. https://doi.org/10.1016/j.coldregions.2021.103461.

[30] Helbling C, Karbhari V. Durability of composites in aqueous environments. In: Durab. Compos. Civ. Struct. Appl. Amsterdam, The Netherlands: Elsevier; 2007. p. 31–71.

[31] J. Sena-Cruz, P. Fernandes, P. Silva, J. Barros, M.R.F. Coelho, Bond behaviour of concrete elements strengthened with NSM CFRP laminate strips under wet-dry cycles, in: J.W. Cairns, G. Metelli, G. A.Plizzari (Eds.), New Mater. under Sev. Cond., 2012 Publisher creations, 2012.

[32] Garzón-Roca J, Sena-Cruz JM, Fernandes P, Xavier J. Effect of wet-dry cycles on the bond behaviour of concrete elements strengthened with NSM CFRP laminate strips. Compos Struct 2015;132:331–40. https://doi.org/10.1016/j.compstruct.2015.05.053.

[33] Al-Mahmoud F, Mechling JM, Shaban M. Bond strength of different strengthening systems - Concrete elements under freeze-thaw cycles and salt water immersion exposure. Constr Build Mater 2014;70:399–409. https://doi.org/10.1016/j.conbuildmat.2014.07.039.

[34] A. Dushimimana, L. Correia, R. Cruz, S. Cabral-fonseca, J.M. Pereira, J. Sena-Cruz, Durability of CFRP-concrete bond and corresponding involved materials under different natural environmental exposures for a period of four years, in: FRPRCS-15 and APFIS-2022, Shenzhen, China, 2022: pp. 10–14.

[35] A. Dushimimana, L. Correia, R. Cruz, J.M. Pereira, J. Sena-Cruz, Durability of CFRP-Concrete Bond in EBR and NSM Sysytems under Natural Ageing for a Period of Three Years, in: Proc. 20th Eur. Conf. Compos. Mater., CC BY-NC 4.0, Lausanne, Switzerland, 2022: pp. 1–8. 10.5075/epfl-298799_978-2-9701614-0-0.

[36] Committee 440, Guide for the Design and Construction of Externally Bonded FRP Systems for Strengthening Concrete Structures, Farmington Hills, MI, USA, 2017.

[37] CNR-DT 200 R1, Guide for the Design and Construction of Externally Bonded FRP Systems for Strengthening Existing Structures; CNR-DT 200 R1/2013;, Rome, Italy, 2013.

[38] IPQ, IPQ (Instituto Português da Qualidade). 1992. NP EN EN 1992-1-1. Eurocode 2: design of concrete structures - Part 1-1: general rules and rules for buildings, Instituto Português da Qualidade (IPQ)., Caparica, Portugal, 2010.

[39] S&P, S&P 220 Resin epoxy adhesive. Technical Data Sheet, Seewen, Switzerland, 2015.

[40] S&P, S&P CFRP Laminates. Technical Datasheet, Seewen, Switzerland, 2014.

[41] EN 1992-1-1 Eurocode 2, Design of concrete structures - Part 1-1 : General rules and rules for buildings, Brussels, Belgium:, 2004. EN 1992-1-1:2004 (E).

[42] Cruz R, Correia L, Cabral-Fonseca S, Sena-Cruz J. Durability of bond of EBR CFRP laminates to concrete under real-time field exposure and laboratory accelerated ageing. Constr Build Mater 2023;377. https://doi.org/10.1016/j.conbuildmat.2023.131047.

[43] IPQ, IPQ (Instituto Português da Qualidade). 2013. NP EN 12390-13. Testing Hardened Concrete. Part 13: Determination of Secant Modulus of Elasticity in Compression, Instituto Português da Qualidade (IPQ)., Caparica, Portugal, 2013.

[44] IPQ, 2011. NP EN 12390-3. Testing Hardened Concrete. Part 3: Compressive Strength of Test Specimen, Instituto Português da Qualidade (IPQ), Caparica, Portugal, 2011.

[45] BSI, BSI (British Standards Institution). Products and systems for the pro- tection and repair ofconcrete structures – Test methods – Measurement ofbond strength by pull-off. EN 1542., London: BSI, 1999.

[46] ISO, ISO 527-2:2012—Plastics—Determination of Tensile Properties—Part 2: Test conditions for Moulding and Extrusion Plastics, Genève, Switzerland, 2012.

[47] ISO, ISO 527-5:2009 Part 5: Test Conditions for Unidirectional Fibre-Reinforced Plastic composites. Plastic—Determ. Tensile Prop., Inte Genève, Switzerland, 2009; Volume 1, 2009.

[48] Hills TP, Gordon F, Florin NH, Fennell PS. Statistical analysis of the carbonation rate of concrete. Cem Concr Res 2015;72:98–107. https://doi.org/10.1016/j.cemconres.2015.02.007.

[49] Bouzoubaâ N, Bilodeau A, Tamtsia B, Foo S. Carbonation of fly ash concrete: Laboratory and field data. Can J Civ Eng 2010;37:1535–49. https://doi.org/10.1139/L10-081.

[50] Jiang L, Zhang Y. Analysis and calculation of the length of half – carbonated zone in concrete [in Chinese]. Ind Constr 1999;29:4–8.

[51] Tseng H, Hsia J. Concrete carbonation and durability prediction[in Chinese], Hunan Commun. Sci Technol 2006;32:121–6.

[52] Kabir MI, Shrestha R, Samali B. Effects of applied environmental conditions on the pull-out strengths of CFRP-concrete bond. Constr Build Mater 2016;114:817–30. https://doi.org/10.1016/j.conbuildmat.2016.03.195.

[53] Dushimimana A, Niyonsenga AA, Nzamurambaho F. A review on strength development of high performance concrete. Constr Build Mater 2021;307:124865. https://doi.org/10.1016/j.conbuildmat.2021.124865.

[54] Shoukry SN, William GW, Downie B, Riad MY. Effect of moisture and temperature on the mechanical properties of concrete. Constr Build Mater 2011;25:688–96. https://doi.org/10.1016/j.conbuildmat.2010.07.020.

[55] Leone M, Matthys S, Aiello MA. Effect of elevated service temperature on bond between FRP EBR systems and concrete. Compos Part B Eng 2009;40:85–93. https://doi.org/10.1016/j.compositesb.2008.06.004.
[56] Firmo JP, Correia JR, Pitta D, Tiago C, Arruda MRT. Bond behavior between near-surface-mounted CFRP strips and concrete at high temperatures. J Compos Constr 2015;19:04014071. https://doi.org/10.1061/(asce)cc.1943-5614.0000535.
[57] Cruz JS, Barros J. Bond between near-surface mounted carbon-fiber- reinforced polymer laminate strips and concrete. J Compos Constr 2004;82:1513–21. https://doi.org/10.1016/j.compstruc.2004.03.047.